Impact of Cenozoic strike-slip tectonics on the evolution of the northern Levant Basin (offshore Lebanon)

Ramadan Ghalayini, Jean-Marc Daniel, Catherine Homberg, Fadi H. Nader, John E. Comstock

AGU PUBLICATIONS

Tectonics

RESEARCH ARTICLE
10.1002/2014TC003574

Key Points:
- The 3-D seismic data allowed tectonic characterization of the Levant Basin
- Tectonic structures in the Levant Basin are inherited and reactivated
- No active shortening is currently attested offshore Lebanon

Correspondence to:
R. Ghalayini,
ramadan.ghalayini@ifpen.fr

Citation:
Ghalayini, R., J.-M. Daniel, C. Homberg, F. H. Nader, and J. E. Comstock (2014), Impact of Cenozoic strike-slip tectonics on the evolution of the northern Levant Basin (offshore Lebanon), *Tectonics*, *33*, doi:10.1002/2014TC003574.

Received 28 FEB 2014
Accepted 5 OCT 2014
Accepted article online 8 OCT 2014

Impact of Cenozoic strike-slip tectonics on the evolution of the northern Levant Basin (offshore Lebanon)

Ramadan Ghalayini[1,2,3], Jean-Marc Daniel[3], Catherine Homberg[1,2], Fadi H. Nader[3], and John E. Comstock[4]

[1]Sorbonne Universités, UPMC Université Paris 06, Paris, France, [2]CNRS, Paris, France, [3]IFP Energies nouvelles, Rueil-Malmaison, France, [4]Petroleum Geo-Services, Oslo, Norway

Abstract Sedimentary basins adjacent to plate boundaries contain key tectonic and stratigraphic elements to understand how stress is transmitted through plates. The Levant Basin is a place of choice to study such elements because it flanks the Levant Fracture System and the Africa/Anatolia boundary. This paper uses new high-quality 3-D seismic reflection data to unravel the tectonic evolution of the margin of this basin during the Cenozoic, the period corresponding to the formation of the Levant Fracture System, part of the Africa/Arabia plate boundary. Four major groups of structures are identified in the interpreted Cenozoic units: NW-SE striking normal faults, NNE-SSW striking thrust-faults, ENE-WSW striking dextral strike-slip faults, and NNE trending anticlines. We demonstrate that all structures, apart of the NW-SE striking normal faults, are inherited from Mesozoic faults. Their reactivation and associated folding started during the late Miocene prior to the Messinian salinity crisis due to a NW-SE compressional stress field. No clear evidence of shortening at present-day offshore Lebanon and no large NNE-SSW strike-slip faults parallel to the restraining bend are found indicating that the Levant Fracture System is mainly contained onshore at present day. The intermittent activity of the interpreted structures correlates with the two stages of Levant Fracture System movement during late Miocene and Pliocene. This paper provides a good example of the impact of the evolution of plate boundaries on adjacent basins and indicates that any changes in the stress field, as controlled by the plate boundary, will affect immediately the preexisting structures in adjacent basins.

1. Introduction

Crustal structures related to transform plate boundaries have been extensively documented worldwide [e.g., *Woodcock*, 1986; *Sylvester*, 1988; *Cunningham and Mann*, 2007]. Relative displacements at this type of plate boundary are accommodated by complex fault systems that have been classified in detail (see *Dooley and Schreurs* [2012] for a review) and that can locally create restraining or releasing bends [e.g., *Cunningham and Mann*, 2007] forming typical strike-slip basins [*Mann et al.*, 1983] bound by subparallel master faults [*Sylvester*, 1988]. Considerable efforts have been concentrated on the study of the boundary itself [*Freund*, 1974; *Zoback*, 1991], while little attention has been paid on the impact of such fault systems on adjacent basins. Hence, studying such areas should provide some understanding on how stress and strain are transmitted to the plate interiors from transform plate boundaries.

The eastern Mediterranean Levant Basin is an area where the effect of an adjacent major strike-slip fault in a complex geodynamical context can be tested. The Levant Basin is today bordered by the Levant Fracture System (LFS) to the east, a 1000 km long left-lateral transform fault, linking rifting in the south with collision and suturing in the north (Figure 1). Extensive work over the evolution of the LFS was conducted previously, leading to a wealth of knowledge regarding its evolution. However, lack of offshore data in past years and uncertainty regarding geometry, displacement, and shortening over the LFS onshore has led to major debates on the geological evolution of the Levant margin, in general (see *Beydoun* [1999] for a review), and the Lebanese restraining bend in particular [*Butler et al.*, 1998; *Walley*, 1998; *Gomez et al.*, 2007b; *Homberg et al.*, 2010]. Certain authors argue that deformation continues offshore where shortening occurred along NNE-SSW structures [*Elias et al.*, 2007; *Carton et al.*, 2009]. There are also unexpected aspects of the deformation in Lebanon like the decrease of shortening onshore since Pliocene time [*Homberg et al.*, 2010], whereas plate kinematics predict an increase in the transpressive character of the plate motion

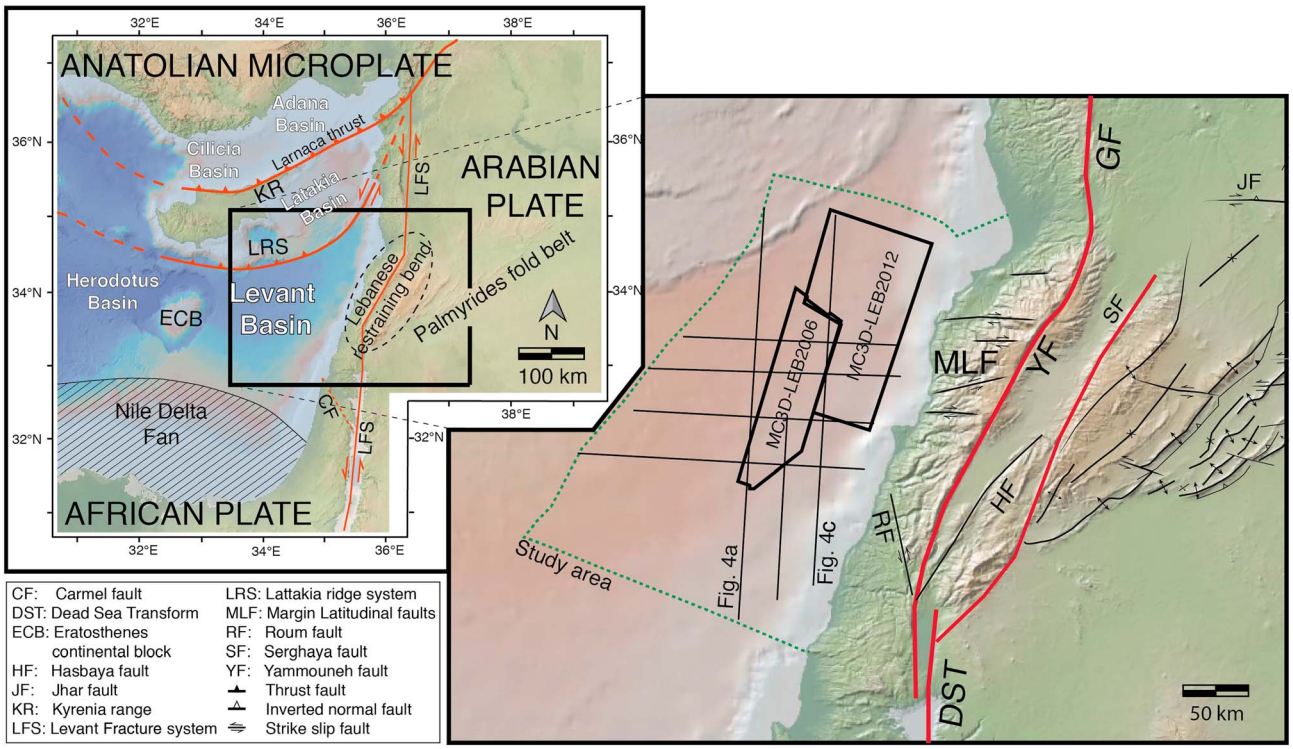

Figure 1. Location map of the study area showing the major structures of the eastern Mediterranean and the data set available for this study. Background map is from http://www.geomapapp.org.

[*Le Pichon and Gaulier*, 1988]. The interpretation of the structures in the Levant Basin is also challenging due to the complex tectonic setting characterizing this basin since the Late Mesozoic.

Recent high-quality 3-D seismic reflection data permit a detailed study of the northern Levant Basin, offshore Lebanon. The availability of such data allowed to better constrain and understand the stratigraphy and geodynamics offshore Lebanon [*Montadert et al.*, 2010, 2013; *Hawie et al.*, 2013b]. In this paper, detailed interpretation of the new 3-D seismic data unveiled the structural evolution of the northern Levant Basin during the Cenozoic and the effects of the nearby LFS. The described structures offshore Lebanon are then correlated with the regional tectonics of the Levant Basin in order to investigate causative mechanisms during their formation and growth.

2. Regional Setting

The Levant Basin (Figure 1) formed due to pulsed breakup of Gondwana during the Late Paleozoic to Mesozoic [*Garfunkel and Derin*, 1984; *Robertson*, 1998]. The strongest pulse is believed to have occurred during the Early to Middle Jurassic [*Ben-Avraham et al.*, 2002]. Numerous NE-SW striking Mesozoic normal faults were perpendicular to the rifting, which occurred under a NW-SE extensional direction [*Gardosh et al.*, 2010; *Montadert et al.*, 2013]. Seismic refraction profiles in the eastern Mediterranean [*Makris et al.*, 1983; *Ben-Avraham et al.*, 2002; *Netzeband et al.*, 2006] may indicate that the crust is only 8 km thick and thus significantly thinned beneath the Levant Basin [*Hirsch et al.*, 1995; *Vidal et al.*, 2000; *Gardosh et al.*, 2010]. Onshore gravity data demonstrate the westward thinning of the continental crust beneath Syria and Lebanon [*Beydoun*, 1977; *Khair et al.*, 1997], and seismic refraction data show a similar trend in Israel and its offshore [*Makris et al.*, 1983; *Netzeband et al.*, 2006]. Inland, the Palmyra Basin has been an important sedimentary depocenter since the Late Permian [*Brew et al.*, 2001] and Triassic [*Chaimov et al.*, 1992] with extension and normal faulting in the Jurassic and Late Cretaceous [*Best et al.*, 1993; *Chaimov et al.*, 1993; *Litak et al.*, 1998]. Lebanon and its offshore might constitute the westward continuation of the Palmyra Basin [*Walley*, 1998].

During the Late Cretaceous, subduction and obduction accommodated progressive closure of the Neo-Tethys ocean [*Stampfli and Hochard*, 2009; *Frizon de Lamotte et al.*, 2011]. This major geodynamic event also caused the contraction of the Levant Basin and margin and triggered the development of an arcuate fold belt

in Palmyra, Israel, and Sinai, termed the Syrian Arc [*Walley*, 1998]. This fold belt resulted from the inversion of Early Mesozoic extensional structures [*Druckman*, 1981; *Best et al.*, 1993; *Chaimov et al.*, 1993; *Druckman et al.*, 1995]. Two main episodes of Syrian Arc folding have been identified: Early Senonian and late Eocene/Oligocene [*Hempton*, 1987; *Moustafa and Khalil*, 1994; *Eyal*, 1996; *Garfunkel*, 1998; *Walley*, 1998].

Collision of and suturing between Afro-Arabia and Eurasia commenced during the Oligocene to early Miocene [*Dewey et al.*, 1973; *Sengor and Yilmaz*, 1981; *Beydoun*, 1993; *Allen et al.*, 2004; *Frizon de Lamotte et al.*, 2011]. It resulted in the formation of numerous trending NE-SW gentle folds, both onshore and offshore. Similarly, angular unconformities between the middle Eocene and Burdigalian in Lebanon [*Dubertret*, 1955; *Walley*, 1998; *Boudagher-fadel and Clark*, 2006; *Homberg et al.*, 2010; *Hawie et al.*, 2013a], NW Syria, and the Palmyra Basin [*Sawaf et al.*, 2001] attest together with these NE-SW anticlines to a regional folding during the early Miocene.

The Oligocene to early Miocene has witnessed the separation of Arabia from Africa. This has resulted in the establishment of a new plate boundary along the Red Sea and the present location of the LFS (Figure 1) [*Le Pichon and Gaulier*, 1988]. The LFS is a series of predominantly strike-slip faults cutting the NW Arabian margin between the Gulf of Aqaba in Jordan and the Taurus Mountains in Turkey. It forms a 1000 km long, left-lateral transform system [*Dubertret*, 1955; *Quennell*, 1958] comprising, from south to north, the N-S Dead Sea segment, the NNE-SSW striking central segment in Lebanon, and the N-S Ghab Fault (Figure 1) [*Quennell*, 1958; *Freund*, 1965; *Dubertret*, 1972]. The central LFS segment in Lebanon forms a restraining bend with many strike-slip faults and folds, comprising the NNE-SSW striking Yammouneh and Serghaya Faults [*Dubertret*, 1955] (Figure 1). Deformation within the LFS restraining bend is mainly partitioned along its different structures [*Gomez et al.*, 2007b]. Part of those structures consist of ENE-WSW to E-W faults crosscutting the Lebanese margin and termed the latitudinal faults [*Gedeon*, 1999]. These faults are dextral strike slip with offsets of about 1–2 km, seismically active, and are widely recognized as reactivated Mesozoic structures, potentially extending to the offshore [*Dubertret*, 1955; *Sabbagh*, 1961; *Gedeon*, 1999]. The potential offshore expression of the LFS forms part of the focus of this paper. *Ron et al.* [1984] explain the occurrence of the dextral strike-slip faults as contemporaneous with block rotation caused by sinistral strike-slip faulting along the LFS. Synchronously with movement on the LFS, the Lattakia Ridge System (LRS) was active and accommodating during the Messinian and Pliocene sinistral strike-slip movement between Cyprus and the eastern Levant margin. This activity was associated with westward escape of the Anatolian microplate, relative to the Eurasian Plate, following a counterclockwise direction of rotation [*Sengor and Yilmaz*, 1981; *Hall et al.*, 2005; *Reilinger et al.*, 2006; *Le Pichon and Kreamer*, 2010].

3. Data Set and Methodology

The study area covers the northern Levant Basin, offshore Lebanon between 33°N and 35°N (Figure 1). Two seismic cubes are used in this study, courtesy of Petroleum Geo-Services (PGS): (i) 1516 km^2 prestack time-migrated (PSTM) MC3D-LEB2006, which was acquired in 2006 using six streamers and two 3090 cubic inch air guns positioned at a depth of 6 m in water depth ranging between 1.5 and 2 km. Streamer length was 6000 m long at a spacing of 12.5 m and 25 m shot point intervals; and (ii) 2774 km^2 PSDM MC3D-LEB2012, which was acquired in 2012 using 12 streamers and two 4135 cubic inch air guns positioned at a depth of 6 m in water depth ranging between 1.5 and 2 km. Streamer length was 7050 m long at a spacing of 12.5 m and 25 m shot point intervals. In addition, 830 km long seven N-S regional 2-D seismic lines were also provided by PGS and acquired in 2008 using a 6180 cubic inch air gun at 8 m and 8100 m long streamer with 9.2 s recording length (Figure 1).

The presence of a 2 km thick salt unit in the basin [*Hsu et al.*, 1973] creates significant velocity anomalies in underlying units. Furthermore, the structural complexity of the Levant Basin causes variations in lateral velocities. Thus, prestack depth-migrated (PSDM) data, where available, were of great value to this study. PSDM is an efficient way to correct image distortion caused by overburden velocities in reflections and to reduce the effect of lateral velocity variations caused by the complex structural geometries [e.g., *Agudelo et al.*, 2009].

The interpretation of detailed structural elements was performed on depth-converted sections. This has helped to negate the interpretation of artifacts related to the thick Messinian evaporites. Because no well data were available, time to depth conversion was done using a velocity model built from stacking velocities. Frequency ranges are between 40 and 80 Hz, yielding a tuning thickness of about 6 m in the Pliocene and 15–25 m in the Miocene. The interpretation workflow included a continuous integration between regional 2-D seismic lines and 3-D seismic cubes. The interpretation of horizons and faults and the creation of isopach maps were

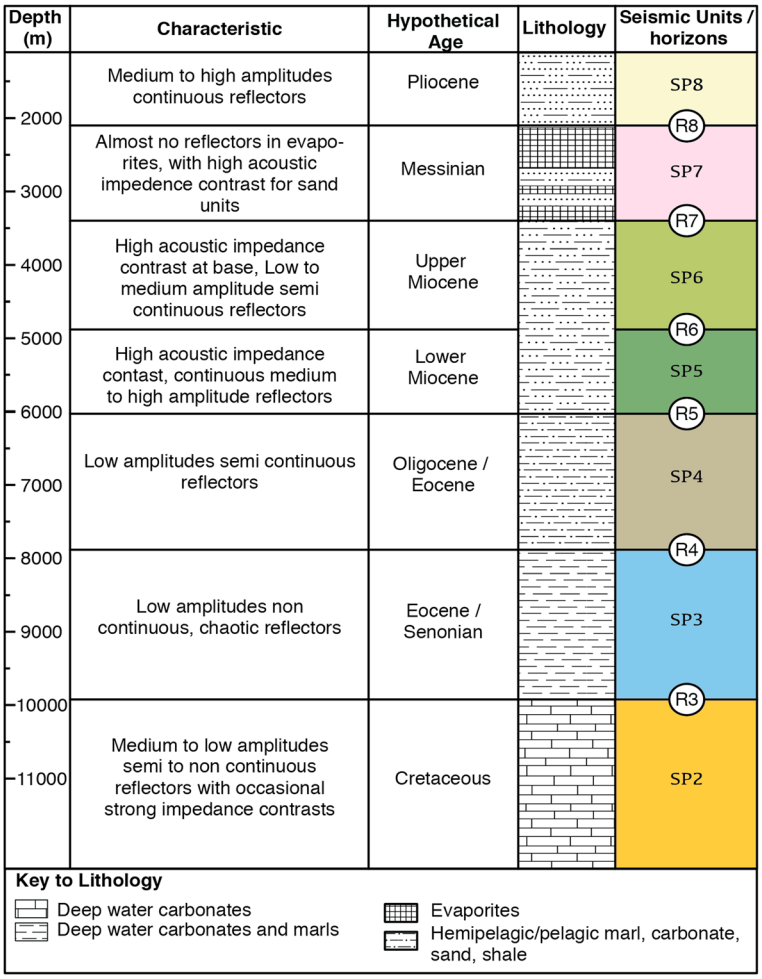

Figure 2. Regional stratigraphic column of the Levant Basin. Seven seismic units are interpreted in this data set consisting of deepwater carbonates and marls SP2 unit; hemipelagic/pelagic sediments SP3 unit; stacked deepwater clastic and hemipelagic deposits SP4, SP5, and SP6; evaporite SP7 unit; and intercalated turbidites/hemipelagic SP8 unit. These seismic sequences are mapped based on the interpretation of seismic packages and their bounding surfaces. Due to lack of drilling activities and well data offshore Lebanon, dating of these packages is based on wells offshore Israel [*Gardosh et al.*, 2006] and thus remains speculative. Nomenclature of units is adopted from *Hawie et al.* [2013b].

performed on 2-D data by using several depth structure maps at different levels, which allowed understanding the geometry of the basin and the distribution of key stratigraphic units (Figure 2). Following this step, detailed interpretation of structural elements was performed using amplitude cubes, structural seismic attributes, and depth structure maps (Figure 5). The attributes used included coherence attributes to image discontinuities and faults [e.g., *Bahorich and Farmer*, 1995], and dip attributes to enhance visualization of anticlines and folds.

4. Structural Style of the Northern Levant Basin

The interpretation of seismic data was used to build the structural scheme illustrated in Figure 3. The main structural elements in the basin can be divided into pre-Cenozoic and Cenozoic structures. The former will not be investigated in detail in this paper due to large uncertainties in the pre-Cenozoic units and the relatively poorer seismic resolution at greater depths.

4.1. Pre-Cenozoic Structures

4.1.1. Description

Regional 2-D seismic lines show the overall geometry of the basin (Figure 4). An important structure named the Saida-Tyr Plateau (STP) is found to the south of the study area (Figure 4). It is bounded to its north by a deep

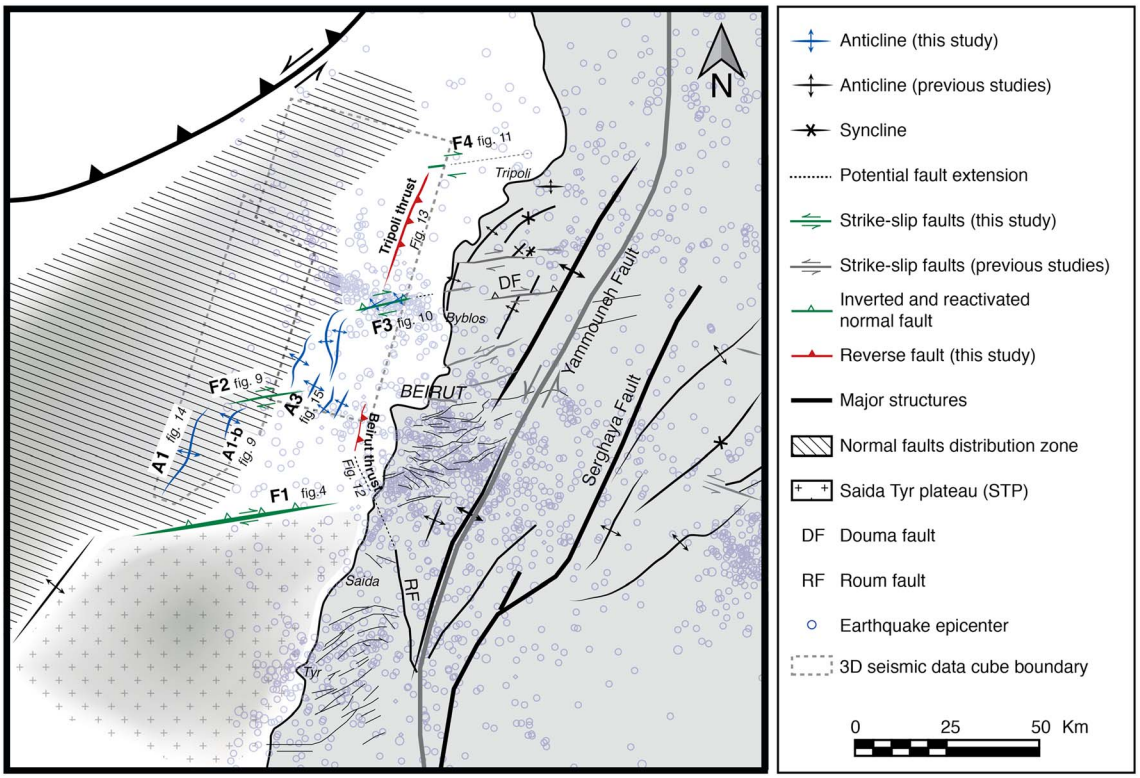

Figure 3. Structural map of the Levant Basin offshore Lebanon showing the structures of the basin, together with the structures onshore in Lebanon and part of Syria. The structures mapped in the course of this study are based on 3-D seismic interpretation and consist of four predominant fault sets: (i) NE-SW trending thrust faults (in red), (ii) ENE-WSW striking dextral strike-slip faults (in green), (iii) NNE trending anticlines (in blue), and (iv) NW-SE striking normal faults (in hachure). Onshore structures are adopted from *Brew et al.* [2001] and *Dubertret* [1955].

crustal fault (F1), separating it from the distal part of the Levant Basin. To its west, it is separated from the thick Cenozoic units by NNE-SSW striking strike-slip faults [*Hawie et al.*, 2013b]. The magnetic maps of the Levant Basin show the presence of an irregular body below the STP, evidenced by relatively stronger magnetic anomalies than its surrounding [e.g., *Segev and Rybakov*, 2010]. The Levant Basin north of STP is characterized by a 9 km thick succession of Cenozoic sediments. SP3 and SP4 units (interpreted as Senonian/Eocene and Oligocene) thicken to the north, whereas units SP5 and SP6 (interpreted as lower and upper Miocene) thicken toward the basin center (Figure 4).

In the NW part of the study area, the LRS marks the northern boundary of the Levant Basin (Figure 4). LRS forms a fold and thrust belt, with a vertical cumulated displacement of Tertiary strata of about 3 km and comprises many deep thrust faults, ramp anticlines, hanging wall cutoffs, and growth strata architecture. It affects all the units in the basin, from the Cretaceous until Pliocene and marks a prominent topography at the seafloor.

4.1.2. Interpretation

The relatively thinner Miocene units on top of STP indicate that the latter was in place during the Cenozoic when the Miocene sediments were deposited. Furthermore, the geophysical and structural observations over STP indicate that this structure might be an old fragment of a thick continental crust bordered by faults. The crustal thickness below STP is larger than the rest of the basin, and hence, it might resemble the Eratosthenes Seamount [e.g., *Makris et al.*, 1983].

The variations of thicknesses of Tertiary units in the basin indicate a certain geodynamic control prior to and during the Cenozoic, shaping the current architecture of the basin. The thickening of SP3 (Senonian/Eocene) and SP4 (Eocene/Oligocene) is observed close to the LRS [*Hawie et al.*, 2013b] and indicates active subduction in the Upper Cretaceous [*Hall et al.*, 2005] (Figure 4). The thickening of the Miocene units (SP5 and SP6) suggests a geodynamic change during the Miocene responsible in shifting the sedimentary depocenter toward the center of the basin, after being closer to LRS in the Senonian and Eocene.

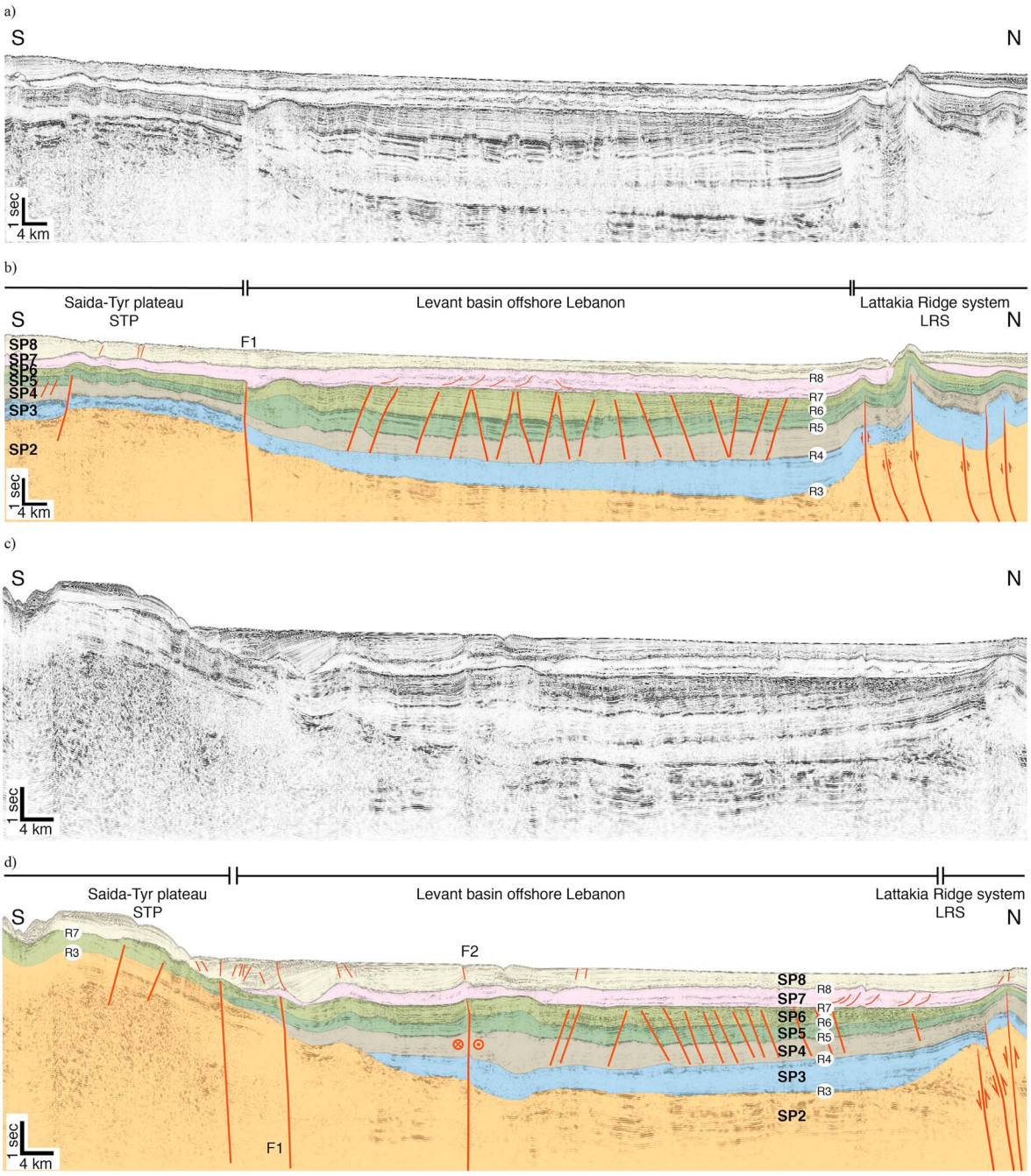

Figure 4. Regional N-S 2-D seismic sections across the Levant Basin offshore Lebanon showing the different structural and stratigraphic elements of the basin, delimited by the Lattakia Ridge System to the north and by the Saida-Tyr Plateau to the south. For location, see Figure 1.

4.2. Cenozoic Structures

A depth-structure map of the mid-Miocene horizon (R6) and a depth slice in the dip attribute cube near the base-Messinian horizon (R7) show the presence of several anticlines and faults (Figure 5). The geometry, age and relationship between these structures, can be studied in detail with the available 3-D seismic data (Figures 3–5). Overall, four different groups of structures are identified (Figure 3), and these are described below.

4.2.1. Normal Faults

4.2.1.1. Description

A dense array of normal faults is found in the central, deepest part of the Levant Basin (Figures 3–6). These faults are regularly spaced and typically strike NW-SE. They dip 60° either to the NE or SW. Furthermore, they

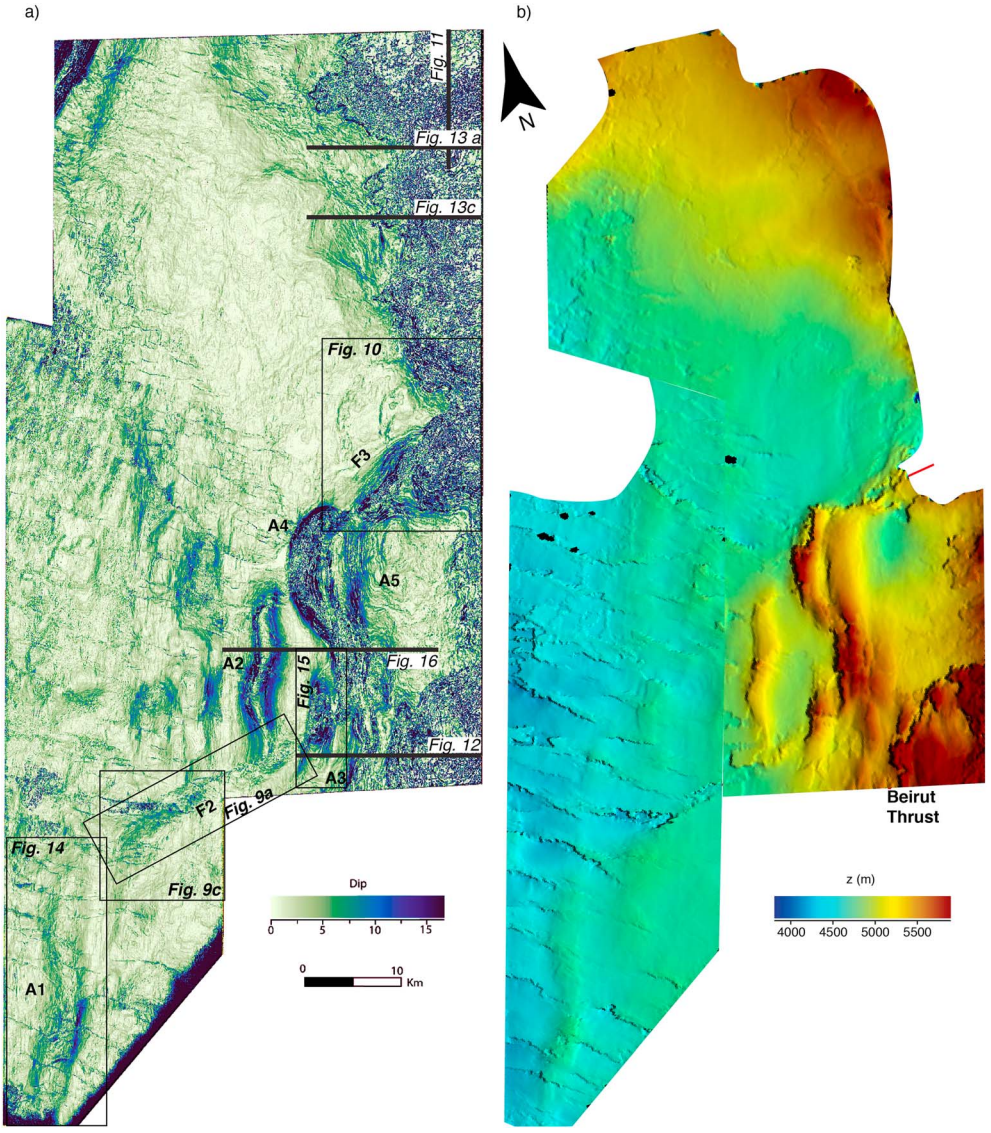

Figure 5. (a) Depth slice in the dip attribute cube taken below R7 horizon along the MC3D-LEB2006 and MC3D-LEB2012 seismic cubes and (b) depth structure map of R6 (base mid-Miocene horizon). These maps show the multitude of folds and faults in the Levant Basin offshore Lebanon and their distribution. The boundary and location of the 3-D blocks are shown in Figure 1.

are layer bound, being developed only in the Oligocene-Miocene units (SP4, SP5, and SP6) and bounded above and below by the interpreted base Messinian (R7) and Eocene unconformity (R4) (Figures 4–6). The maximum documented displacement along these faults is 415 m. Superposition of a basin-wide fault mapping [*Dupin et al.*, 2012] and a Miocene isopach revealed that these faults are tallest and have highest displacement, where the Miocene sequence is relatively thick (Figure 7). They are almost absent along the margin of the basin and on the STP and are less well developed in the southern Levant Basin, where the Miocene unit is thinner [e.g., *Gardosh and Druckman*, 2006]. Sediment thickness calculations for units belonging to lower and upper Miocene (SP5 and SP6, respectively) along fault planes revealed expansion index ratio as defined by *Cartwright et al.* [1998] between 1.02 and 1.2 (Figure 8).

4.2.1.2. Interpretation

The thickening of units in the hanging wall blocks indicates that these faults have nucleated in the early Miocene. They were synsedimentary during the Miocene, with uncertainty on their current activity. The presence of NW trending normal faults in the basin is not coeval with any documented NE-SW extension during the Miocene in the Levant Basin. It is hence difficult to relate these faults with a tectonic origin. Knowing the

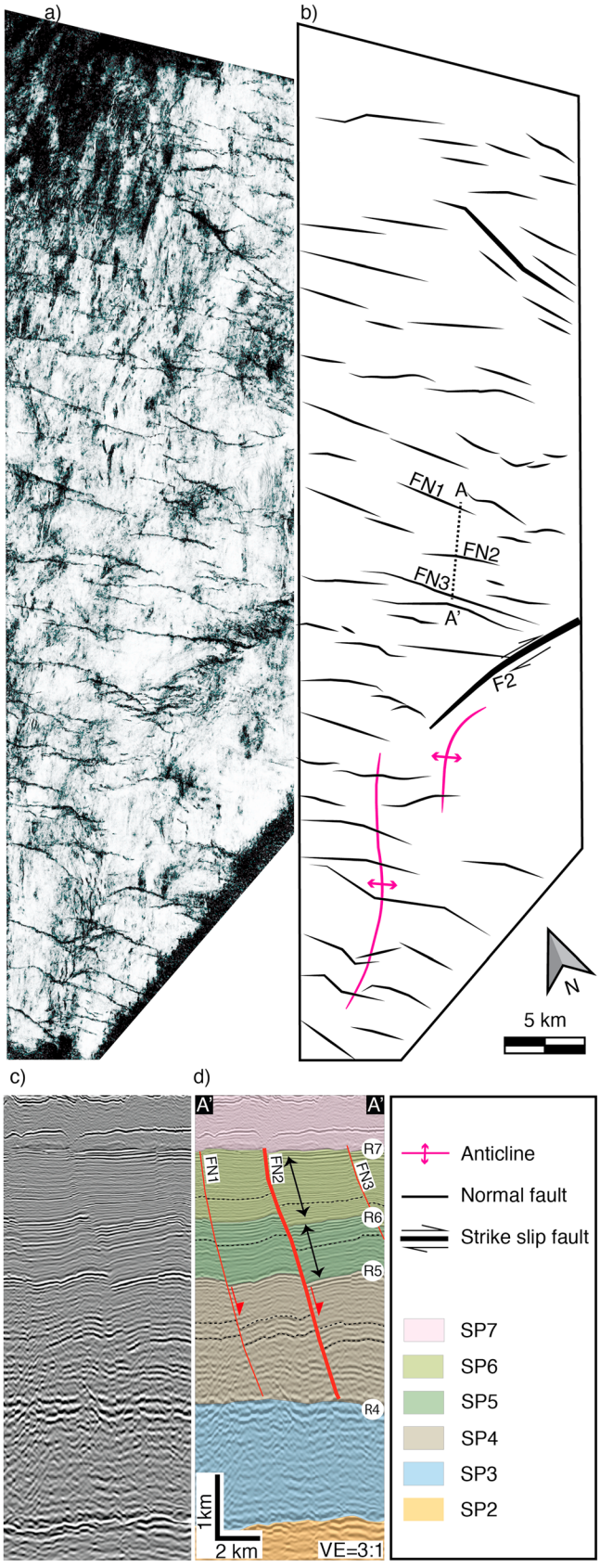

strong correlation between sediment thickness and the distribution of these faults, it is very likely that their distribution might be associated with the thickness of the Miocene units. It is out of the scope of this paper to perform detailed analysis of displacement distribution and variation along the fault planes in order to constrain the temporal and spatial evolution of these faults [*Walsh and Watterson*, 1988].

4.2.2. ENE-WSW Striking Strike-Slip Faults

4.2.2.1. Description

Four parallel ENE-WSW striking faults are observed in 2-D (fault F1) and 3-D data (faults F2, F3, and F4) (Figures 3–5). These faults are nearly vertical and affect all the units from the Cretaceous (SP2) until Messinian (SP7). At seabed, they are associated with localized deformation and faulting (Figures 10 and 11). Fault F1 has a variable throw along its strike, reaching 750 m in places (Figure 4). It is bordering the STP described in previous sections and is only observed in 2-D data in this study, which limits observation and interpretation.

Fault F2 is a 25 km long steep fault that appears locally as a negative flower structure toward the westward tip of the fault (Figure 9e). The vertical throw associated with this fault is variable along its length. In section AA′ and BB′ (Figure 9), R3 (Senonian unconformity horizon) is 500 m displaced downward NW of the fault plane, while the remaining horizons show no displacement. In section BB′, R5, R6, and R7 are 300 m displaced downward SE of the fault (Figure 9f). An erosive surface along the base Messinian horizon (R7) is observed in section AA′ above the

Figure 6. (a) Coherence attribute slice below R7 horizon from MC3D-LEB2006 PSTM seismic cube. (b) Interpretation of the coherence map showing the distribution and orientation of the normal fault array. (c and d) Seismic section across three normal faults showing the thickening of units in the hanging wall block in SP5 and SP6 units along FN2. The arrows in Figure 6d indicate the units on which expansion index (EI) > 1 have been recorded. For the location of the seismic block, see Figure 1.

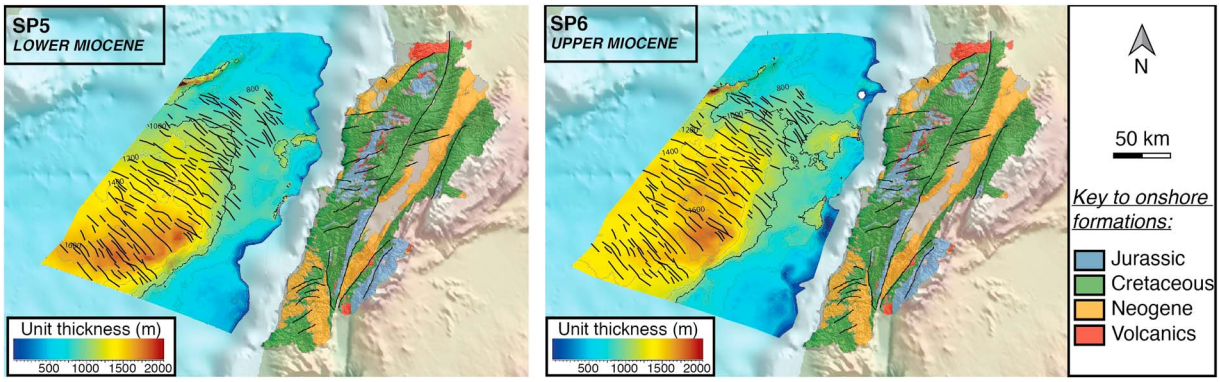

Figure 7. Isopach maps of the lower and upper Miocene with superposed normal fault distribution map in the Levant Basin offshore Lebanon. Basin-wide mapping of the normal fault is taken from *Dupin et al.* [2012].

structure (Figure 9e). In map view (Figures 9b–9d), small scale closely spaced faults oriented at 60° to and crosscut by F2 are observed. These structures consist of small normal faults of 200 m throw that displace the Miocene units (SP5 and SP6) and which branch off on the vertical master fault. The absence of displaced markers does not allow verifying if any strike-slip movement occurred along these faults. An anticline (A1-b) with a 10 km long axis and 200 m fold amplitude is observed adjacent to F2. It is bending 30° clockwise when it approaches the westward tip of F2 (Figure 9d).

Fault F3 is 15 km long and is located closer to the Levant eastern margin than F2 (Figure 3). It consists of a vertical or NW dipping steep fault crosscutting SP2, SP3, SP4, SP5, and SP6 (Cretaceous to upper Miocene units). R3 (Senonian unconformity) and R4 (Eocene unconformity) are displaced downward of 1 km (Figure 10). Reverse drag is observed along R6 (base mid-Miocene horizon) in both the footwall and the hanging wall. In the footwall, the Oligocene/Eocene unit (SP4) is significantly reduced or absent, overlying a clear erosional surface along R4 (Eocene unconformity), and the top of the upper Miocene unit (SP6) is eroded and truncated (Figure 10d). In SP6, two parallel 6 km long anticlines are crosscut by F3 and oriented 60° from the F3 fault plane (Figure 10b). On top of F3, the Messinian is folded, and gentle uplift and deformation are observed in SP8 (Pliocene).

Fault F4 can only be seen in a small area in the northeastern side of the MC3D-LEB2012 seismic survey (Figure 3). It consists of a nearly vertical fault, with a displacement of 750 m of Cretaceous horizons (within SP2) (Figure 11). SP8 (Pliocene unit) is severely deformed by this fault, and the seabed is vertically displaced for about 500 m. The erosion and truncation of R2 (Senonian unconformity horizon) are recorded in the hanging wall. A significant hiatus is observed along this fault and includes the Eocene, Oligocene, Miocene, and Messinian units (SP3 to SP7) (Figure 11).

4.2.2.2. Interpretation

The ENE-WSW striking structures are believed to be dextral strike-slip faults, based on the following arguments: (i) the faults are narrow, nearly vertical and thoroughgoing; (ii) abrupt thickness changes in correlative stratigraphic units across fault planes (Figures 4, 9, 10, and 11); (iii) passive eastward bending of anticlinal axis close to F2 (Figure 9), (iv) shallow splay faults resembling Riedel-like structures at 60° from F2 and converging at depth into a steep fault zone (Figure 9); (v) en echelon alignment of two anticlines in the upper Miocene oriented at 60° from the F3 fault plane (Figure 10); and (vi) presence of dextral strike-slip faults onshore with same strike (Figure 3) [*Dubertret*, 1955; *Gedeon*, 1999].

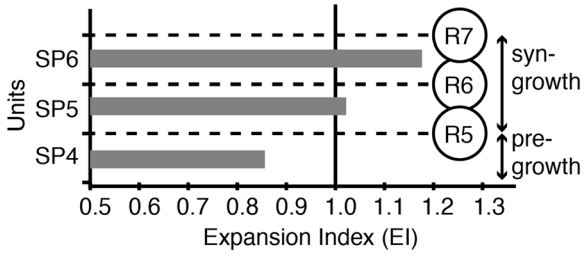

Figure 8. Expansion index plot for one Oligocene-Miocene normal fault. The black vertical line indicates the EI values of 1. Value <1 or >1 implies the stratigraphic thinning or thickening of units in the hanging wall, respectively. In the Levant Basin offshore Lebanon, all normal faults show the thickening of SP5 and SP6 (lower and upper Miocene) in the hanging wall, indicating synsedimentary faulting during the Miocene.

The timing of activity of these faults is not straightforward. In F2, no onlap or growth strata in the pre-Messinian packages can be observed to date this fault. The erosion of parts

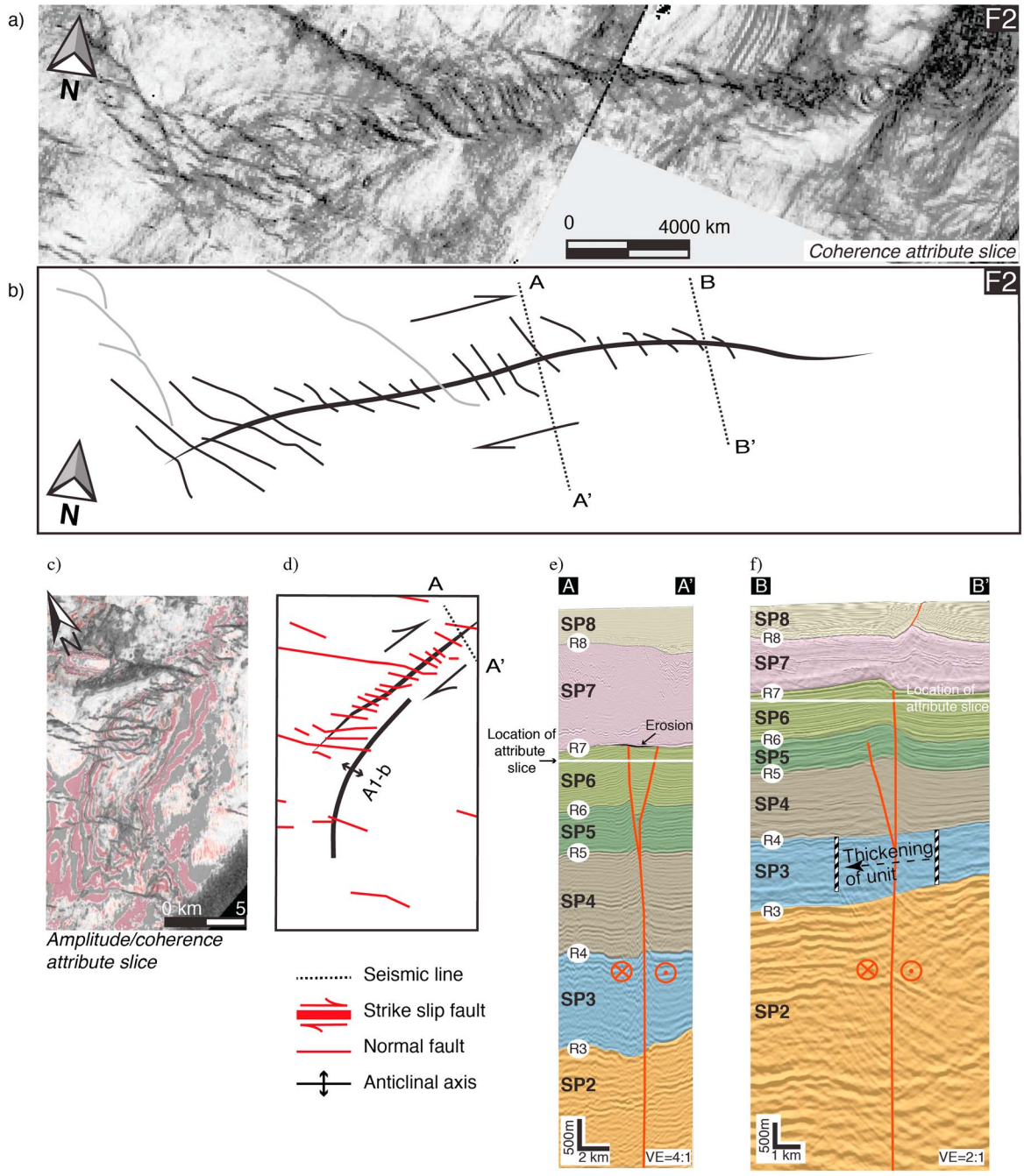

Figure 9. (a and b) Coherence slice below R7 horizon (base Messinian) showing fault F2 along MC3D-LEB2006 and MC3D-LEB2012 seismic cubes, together with the numerous normal faults along the plane of fault F2. (c and d) Merged amplitude and coherence attribute slice below R7 horizon in MC3D-LEB2006 seismic cube, showing the location of an anticline bending to the east. (e and f) Interpreted seismic sections along the strike-slip fault. For location, see Figures 3 and 5.

of the base Messinian horizon (R7) along F2 suggests that the latter was active prior to the Messinian event. In contrast, F3 shows evidence for an even older activity during the Oligocene. The Oligocene hiatus observed in the hanging wall is an indication that the Oligocene unit (SP4) is synkinematic and that F3 was active during this time, probably as a normal fault. As presented above, the F1 Fault borders the northern part of STP, which is a crustal element with different crustal properties. Hence, the faults bounding it might also consist of deep crustal faults. We thus suggest that F1 is an inherited crustal fault nucleated during Mesozoic extension. Superposition of earthquake data (www.cnrs.edu.lb) reveals significant seismicity in the area

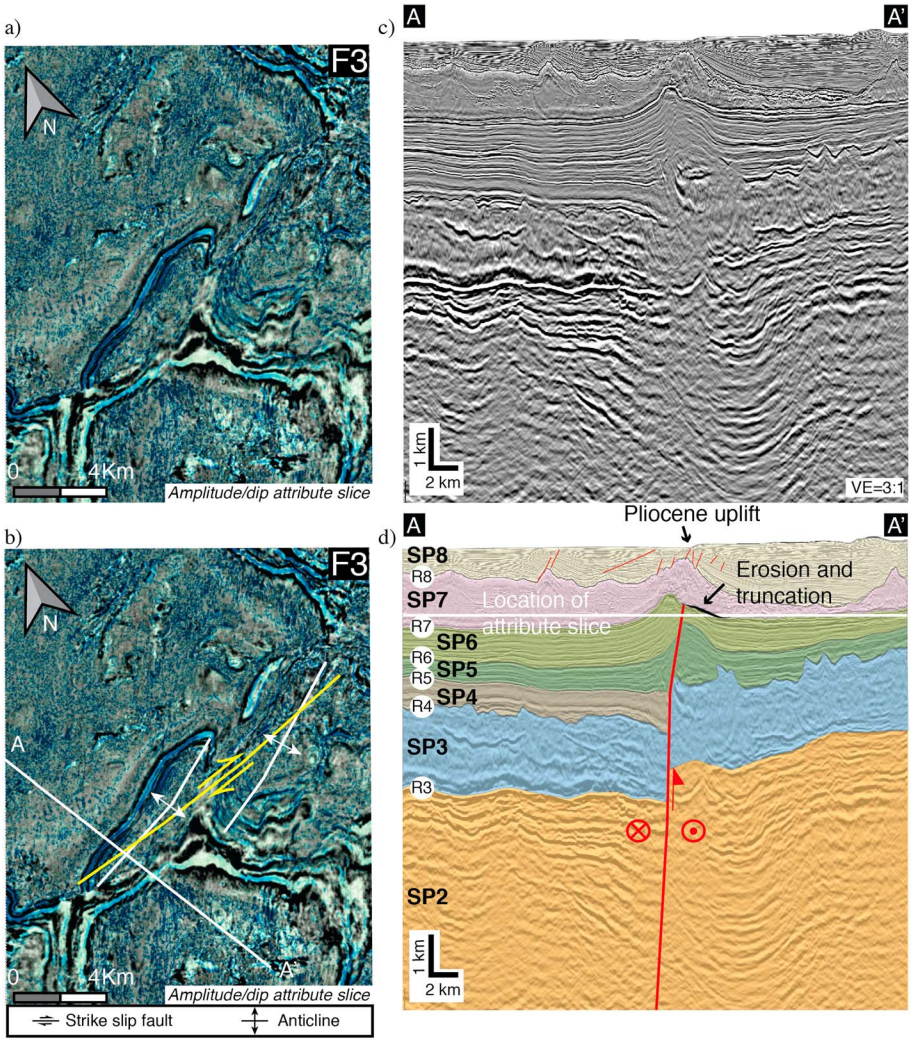

Figure 10. (a and b) Merged amplitude and dip attributes slice of fault F3 from MC3D-LEB2012 PSDM seismic cube, showing the orientation of two anticlines along the strike-slip fault. (c and d) Seismic profile across the fault, showing the inversion and deformation of seabed. For location, see Figures 3 and 5.

adjacent to F3, attesting to its current ongoing activity (Figure 3). Similarly, F4 displaces the seabed for about 500 m and hence is considered as currently active.

The presence of dextral strike-slip faults on the margin, termed latitudinal faults, with a similar trend suggests that the structures both onshore and offshore are genetically related. It is widely accepted that the margin's latitudinal faults are old structures inherited from previous extensional activities [*Dubertret*, 1955; *Sabbagh*, 1961; *Hancock and Atiya*, 1979; *Gedeon*, 1999]. Thus, by analogy, we can advocate that if several structures offshore (F2 and F3) show similar history, trend, and mechanism as the latitudinal faults onshore, then the rest of the structures offshore (F1 and F4) that show the same trend and inheritance history might also be dextral strike slip. They belong, as such, to the same system of wrench faults prevalent on the Levant margin. We thus advocate that all ENE-WSW strike-slip faults offshore are old inherited structures and still active today, in a similar fashion to onshore strike-slip ENE-WSW latitudinal faults.

4.2.3. Thrust Faults

4.2.3.1. Description

Two thrust faults are mapped in the Levant Basin offshore Lebanon: Beirut Thrust and Tripoli Thrust (Figures 3, 12, and 13).

Beirut Thrust is located at the latitude of the city of Beirut. It is dipping 50° to the east, strikes NNE-SSW, and is crosscutting SP2, SP3, SP4, SP5, and SP6 (Cretaceous to upper Miocene units) (Figure 12). R3 and R4 (Senonian

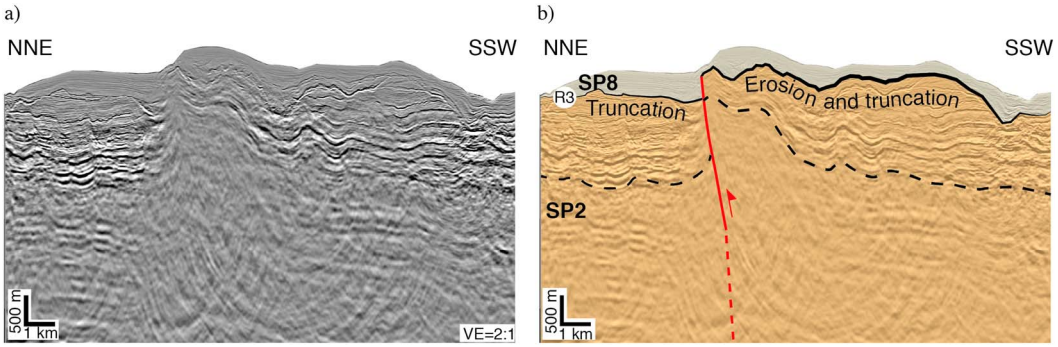

Figure 11. (a and b) Seismic profile across F4 showing a vertical fault affecting units SP2 (Cretaceous) and SP8 (Pliocene), with a vertical displacement up to 750 m. Significant hiatuses of the Eocene, Oligocene, Miocene, and Messinian are observed, together with the erosion and truncation of the Upper Cretaceous. The seabed and Pliocene are uplifted for about 500 m.

and Eocene unconformity horizons) show 2 km vertical displacement along this fault, while R5 (base Miocene) shows only 1 km of vertical displacement. Strong thickness variations are observed along Beirut Thrust in the Oligocene (SP4) and the Eocene (SP3), whereby these units are thinner in the hanging wall (Figure 12). Horizons R6 and R7 (base mid-Miocene and base Messinian horizons) are truncated at the hanging wall of the fault, and part of the upper Miocene (SP6) is absent and eroded (Figure 12c). The fault does not breach the Messinian (SP7); the latter instead is pinching out onto the uplifted hanging wall. The Messinian is observed again toward the East in the hanging wall but is significantly thinner (Figure 12).

Toward the north, another thrust fault is found at the latitude of Tripoli [e.g., *Elias et al.*, 2007; *Carton et al.*, 2009]; this is referred to as the Tripoli Thrust (Figure 13). It is dipping 50° SE and strikes NNE-SSW. It is crosscutting SP2, SP6, and SP7 (Cretaceous, upper Miocene, and Messinian). The Cenozoic units are onlapping on R3 (Senonian unconformity), and hence, SP4 and SP5 are never crosscut by this fault. It is not possible to know the total displacement of R3 (Senonian unconformity) because of the erosion and truncation of the top of SP2 (Cretaceous) in the hanging wall. However, reflectors within SP2 show the displacement of around 3 km, which might be considered as the total displacement in the Cretaceous unit. In contrast, reflectors within the upper Miocene (SP6) are displaced for a maximum of 200 m, while R7 (base Messinian) is only displaced for 100 m in some profiles (Figure 13d). In other profiles, the Messinian is pinching out on Cretaceous units (SP2) (Figure 13b). The overlying Pliocene (SP8) does not seem to be very heavily disturbed and shows minor amount of normal faulting (Figures 13b–13d).

4.2.3.2. Interpretation

The thickness variation of units along Beirut Thrust indicates that the Eocene and the Oligocene are synkinematic (Figure 12d). The erosion of some parts of the Miocene unit does not allow checking whether the fault was active during this time or not by comparing the thickness of units. It is possible to argue that the thickening in units in the footwall of the thrust might be related to global thickening of the Eocene and Oligocene units toward the basin. Although a global thickening toward the basin is generally attested, the thickness change is so abrupt and large along the fault plane that it cannot be related to general thickening of the unit toward the basin. The truncation and erosion of parts of the lower and upper Miocene units indicate that thrusting is pre-Messinian. In the overlying Pliocene unit, small deformation and faulting are related to salt tectonics. A Pliocene sequence is pinching out on a deformed unit, indicating a cessation of Pliocene faulting (Figure 12c). This is explained by the removal of the underlying evaporitic décollement layer, allowing the fault blocks to be welded on the presalt layers and becoming stable as proposed by *Lundin* [1992]. Hence, Pliocene sediments are being deposited today without significant deformation in the hanging wall, which is an evidence for no activity observed along this fault during the Pliocene. The Messinian and Pliocene are hence postkinematic units.

Tripoli Thrust shows similarity with Beirut Thrust. The truncation and erosion of a large part of the top Cretaceous, together with the larger displacement recorded over horizons in the Cretaceous unit compared with the Miocene one (Figure 13), may indicate that this fault was active prior to the deposition of the

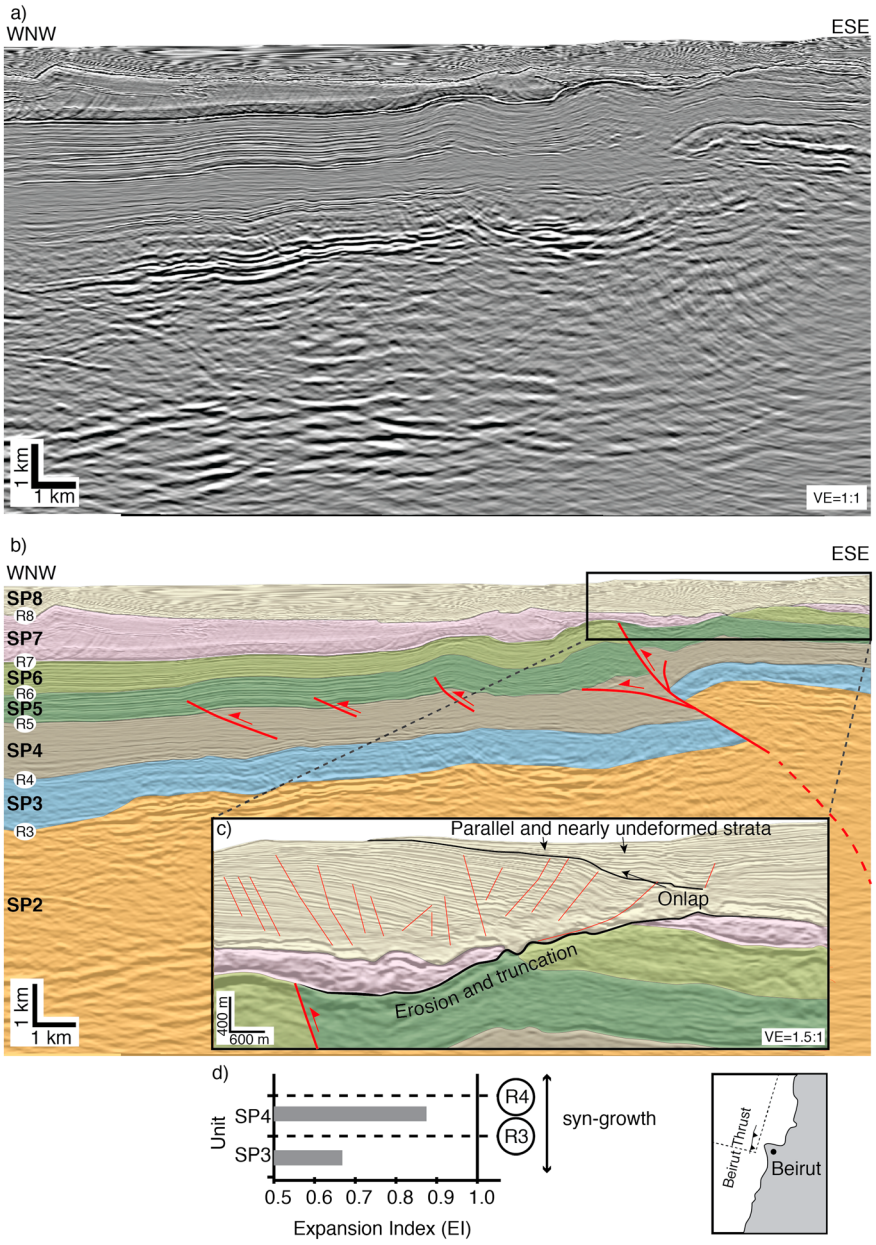

Figure 12. (a and b) Seismic profile across the Beirut Thrust from MC3D-LEB2012 PSDM seismic cube, showing thrusting and uplift. (c) Zoomed section on the top of the hanging wall of the thrust showing potentially a cessation of movement in the Messinian and Pliocene. (d) Expansion index (EI) plot for units SP3 and SP4. The black vertical line indicates the EI values of 1. Value <1 implies the stratigraphic thinning of units in the hanging wall. Because of the erosion of SP5 and SP6 in the hanging wall, no EI plots could be constructed for those units. For location, see Figures 3 and 5.

Miocene unit. It is not possible to determine when faulting started exactly since the Eocene and Oligocene units are not crosscut by the fault, but it is very likely that the major part of deformation took place prior to the Miocene and continued with lesser magnitude during the late Miocene. By analogy to Beirut Thrust, we can advocate that deformation took place in the Late Cretaceous or early Tertiary. The fact that the Messinian is pinching out on the hanging wall and the lack of major deformation and uplift in the Pliocene (Figure 13) indicate that the thrust was inactive during the Messinian and the Pliocene. Indeed, it is hard to consider that large amount of vertical displacement took place during the Messinian or the Pliocene without affecting the Pliocene units, even if the deformation is accommodated by the Messinian salt. The normal faulting observed in the Pliocene is related to salt tectonics similarly to the rest of the margin.

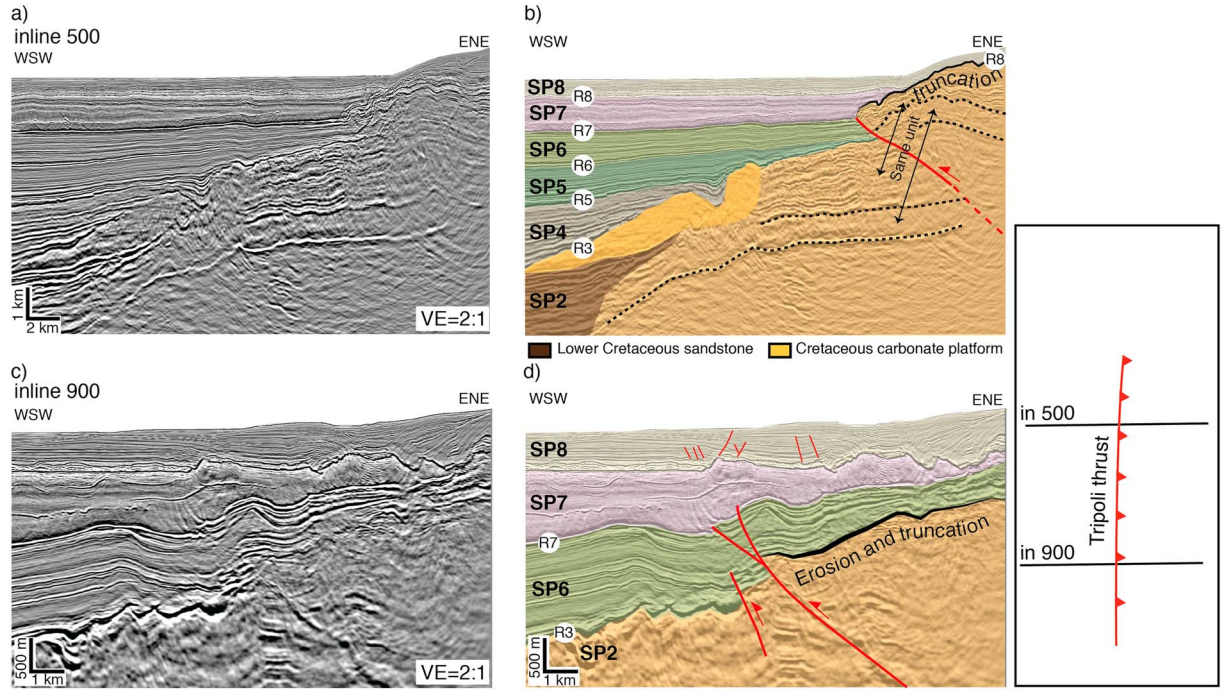

Figure 13. (a–d) Seismic profiles across the Tripoli Thrust offshore northern Lebanon from MC3D-LEB2012 PSDM seismic cube. For location, see Figures 3 and 5.

4.2.4. NNE Trending Anticlines

4.2.4.1. Description

Seven anticlines are mapped in the Levant Basin offshore Lebanon using the available data set. For the purpose of this study, only one anticline "A1" will be described in detail. A1 is located 50 km to the west of Beirut (Figure 3) and is a symmetric fold in map view (Figure 14a). The anticlinal axis is 12 km long trending N28E and is slightly sinuous. The fold amplitude is 350 m. The units affected by this fold are SP4, SP5, and SP6.

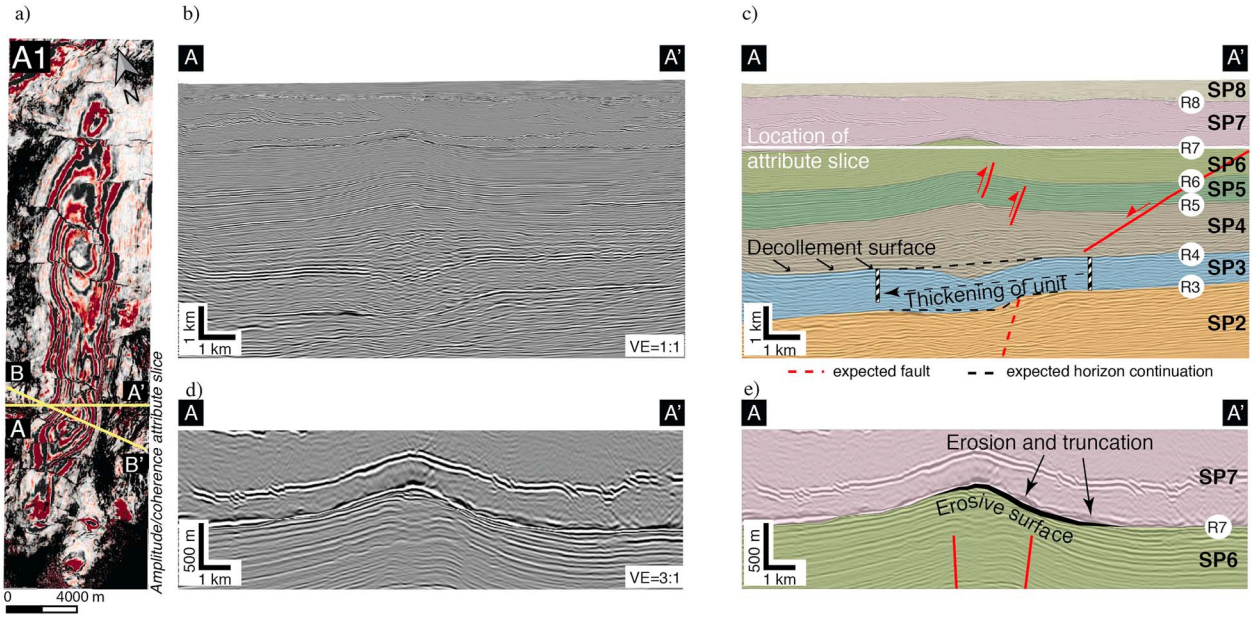

Figure 14. (a) Merged coherence attribute and amplitude slice from MC3D-LEB2006 PSTM seismic cube showing the geometry of the NNE-SSW anticline. (b–e) Seismic profiles across the anticline showing the thickening along SP3 unit and an erosive surface at the anticlinal crest. For location, see Figures 3 and 5.

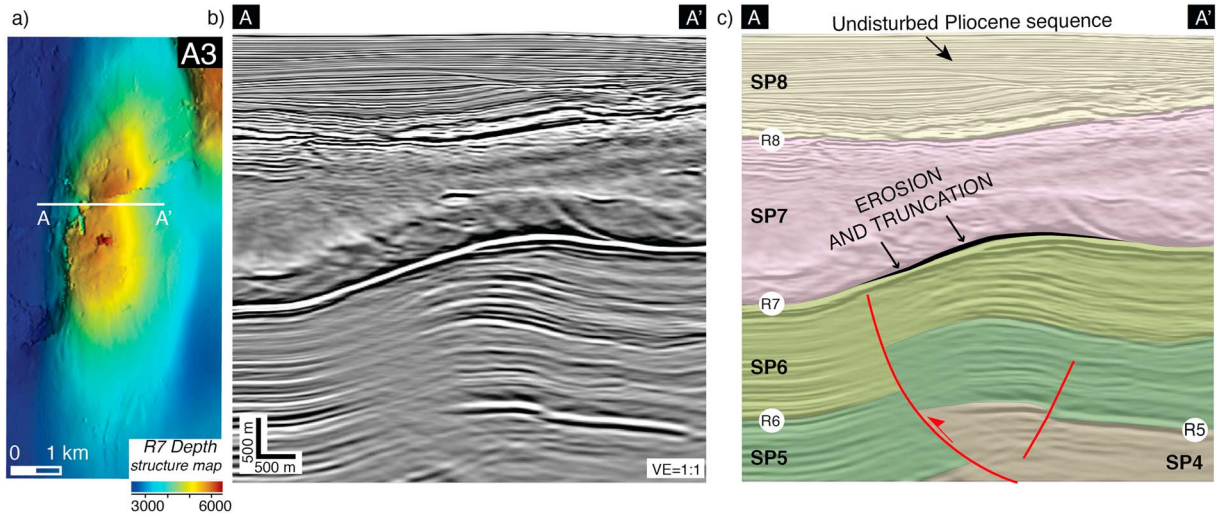

Figure 15. (a) Depth structure map of R7 (base Messinian horizon) from MC3D-LEB2012 PSDM seismic cube showing the geometry of anticline A3. (b and c) Seismic profile across A3 showing the erosion and truncation of R7 horizon. For location, see Figures 3 and 5.

One continuous seismic horizon with strong impedance contrast in SP7 (Messinian) close to R7 (base Messinian horizon) is folded and deformed by the anticline (Figure 14e). In contrast, R3 and R4 (Eocene and Senonian unconformity horizons) are sagging below A1. No thickness variations, onlap, or erosional surfaces can be observed on the flanks of the anticline in the deformed units. However, erosion and truncation along R7 (base Messinian horizon) are documented, and the SP3 (Senonian/Eocene unit) is thickening abruptly west of A1 (Figure 14).

Offshore Beirut, between faults F2 and F3, five other anticlines that detach on R4 are outlined in depth structure and dip attribute maps (Figure 5). All these anticlines are capped by an erosional surface and truncation along the base of the Messinian (R7) (Figure 15) and show no onlap or growth folding along their flanks. In a similar way, all these anticlines are associated with thickness variations of Senonian and Eocene units (SP3 and SP4) toward their western flanks.

4.2.4.2. Interpretation

The sagging of the horizons below anticline A1 constrains the ability to understand the folding mechanisms and geometries. It is possible that this sagging is caused by unexpected velocity anisotropies during seismic imaging and is hence a seismic artifact. We believe that if R3 and R4 had the same fold amplitude as the anticline, then a very strong velocity variation is needed to displace these horizons up to 1 km downward. For this reason, we advocate that R3 and R4 should be flat below the anticline. This would make A1 a detachment fold formed over the Eocene unconformity horizon, which is the décollement surface in this situation.

The erosion and truncation of the crest at the base-Messinian horizon (R7) indicate that this anticline started to grow shortly before Messinian times (Figures 14 and 15). The thickening of the Senonian/Eocene (SP3) and Miocene units (SP5 and SP6) is noticed at the western limb of anticline A1. It denotes the presence of a pre-Eocene paleostructure, possibly active in the Late Cretaceous/early Tertiary. This structure appears to have caused vertical displacement along the Senonian unconformity horizon (R3) responsible for the thickening of the overlying Tertiary units. Hence, it is likely that during the deposition of the Senonian/Eocene units (SP3), a topographic morphology was already in place, which explains the thickening geometries, west of the anticline. The corresponding fault trace cannot be mapped accurately due to velocity problems below the anticline A1. Although it is possible to argue that this thickening is related to bulk westward thickening of the units toward the basin, we believe that the strong and abrupt thickness increase west of the anticline is caused by a preexisting topographic high, or structure, rather than general thickening of units toward the basin. The description of A1 is applicable to the remaining anticlines offshore Beirut as they show the same geometric relationships. We hence advocate that all the anticlines (Figures 3–5) were formed by a similar mechanism and during the same time.

5. Discussion

5.1. Influence of Pre-Cenozoic Structures

Mapping of structures in the Levant Basin offshore Lebanon reveals a number of predominant fault sets: (i) NE-SW trending thrust faults, (ii) ENE-WSW striking dextral strike-slip faults, (iii) NNE trending anticlines, and (iv) NW-SE striking normal faults. With the exception of the NW-SE striking normal faults, all of the structures appear to be inherited and reactivated during the Miocene. Structures such as the ENE-WSW oriented strike-slip faults show reactivation and inversion evidence and most probably are linked to crustal origins. Along the Levant eastern margin in Lebanon, dextral strike-slip faults are aligned with the offshore strike-slip structures documented in this study (Figure 3). It is widely recognized that the onshore latitudinal strike-slip faults are reactivated Mesozoic structures [*Sabbagh*, 1961; *Hancock and Atiya*, 1979; *Ron and Eyal*, 1985; *Nemer*, 1999]. We hence postulate that both of these structures are genetically linked and were initially caused by Mesozoic extension [e.g., *Garfunkel*, 2004; *Gardosh et al.*, 2010; *Homberg et al.*, 2010].

Similarly, NNE-SSW anticlines seem to overly deeper faults or structures in the pre-Tertiary strata (Figure 14). Although such faults cannot be observed accurately in the seismic data due to lower resolution at depth, the thinning and the thickening within the Eocene units suggest a Late Cretaceous structuration (Figure 14). Such thickness variation cannot be attributed to global thickening toward the basin [e.g., *Hawie et al.*, 2013b] because the Eocene units thicken abruptly below the anticlines, which insinuate that existing structuration was affecting sedimentation.

The variability of structural styles in the Levant Basin can be explained in terms of preexisting structuration, influencing the style of current brittle deformation. It is widely acknowledged that fault reactivation is controlled by (i) optimal orientation for frictional slip in the stress field, (ii) size of the fault, (iii) overpressure, and (iv) frictional resistance along the fault plane [*Wiprut and Zoback*, 2002; *Bonini et al.*, 2012]. Hence, a fault is likely to follow a complex history when submitted to several successive states of stress. In the case of the Levant Basin, the various regional geodynamic events, such as the pulsed Mesozoic rifting [*Druckman*, 1984; *Robertson*, 1998; *Barrier and Vrielynck*, 2008; *Gardosh et al.*, 2010], were probably responsible in creating crustal structures. With the subsequent Late Cretaceous to Tertiary subduction, inversion, collision, Anatolian extrusion, and LFS transpression [*Frizon de Lamotte et al.*, 2011], concurrent reorientations of the regional stress field may have caused the reactivation of the preexisting structures into a variety of structural styles. In fact, the inversion of Mesozoic extensional structures has been documented offshore Israel, in the Sinai, and the Palmyrides [*Best et al.*, 1993; *Chaimov et al.*, 1993; *Druckman et al.*, 1995; *Brew et al.*, 2001; *Gardosh and Druckman*, 2006; *Moustafa*, 2010] and is believed to have taken place during the Late Cretaceous and Eocene to early Miocene [*Hempton*, 1987; *Moustafa and Khalil*, 1994; *Eyal*, 1996; *Garfunkel*, 1998; *Walley*, 1998; *Sawaf et al.*, 2001].

5.2. Origin of the NW-SE Normal Fault System

All the structures discussed so far are rooted in pre-Oligocene layers. In contrast, the NW-SE normal faults are Oligocene-Miocene layer bound and die out at the Eocene unconformity horizon (Figures 4–6). In order to tectonically create normal faults in the basin, the maximum principal stress must be vertical. This would be in contrast with the NW trending maximum horizontal stress field prevalent since the Late Cretaceous [*Barrier and Vrielynck*, 2008] that is causing regional shortening and thick-skinned deformation. Since such normal faults are restricted to the Oligocene-Miocene unit, while no NE-SW extension is documented in the Levant Basin at that time, we might speculate that these faults are nontectonic and probably related to the nature of sediments in the host rock unit. The detailed study of the geometry of this fault network and its mechanical origin deserves a specific paper, but it is worth mentioning here that they share many characteristics of polygonal faults systems [e.g., *Cartwright*, 2011] such as (i) layer-bound geometries, (ii) fine-grained sediments in the host unit [*Hawie et al.*, 2013b], (iii) regional extent, and (iv) correlation between their distribution and thickness of the host rock unit.

5.3. Late Cretaceous to Early Tertiary Deformations

The closure of the Neo-Tethys ocean at the onset of the Late Cretaceous has caused inversion, thrusting, and folding throughout the Levant region (e.g., Syrian Arc folds, Palmyrides fold, and thrust belt; cf. Figure 1) [*Hempton*, 1987; *Moustafa and Khalil*, 1994; *Eyal*, 1996; *Garfunkel*, 1998; *Walley*, 1998; *Frizon de Lamotte et al.*, 2011]. The presence of thrust faults offshore Lebanon could fit in this regional geodynamic framework whereby inversion, thrusting, and shortening were dominant. Although there is no indication that Beirut and

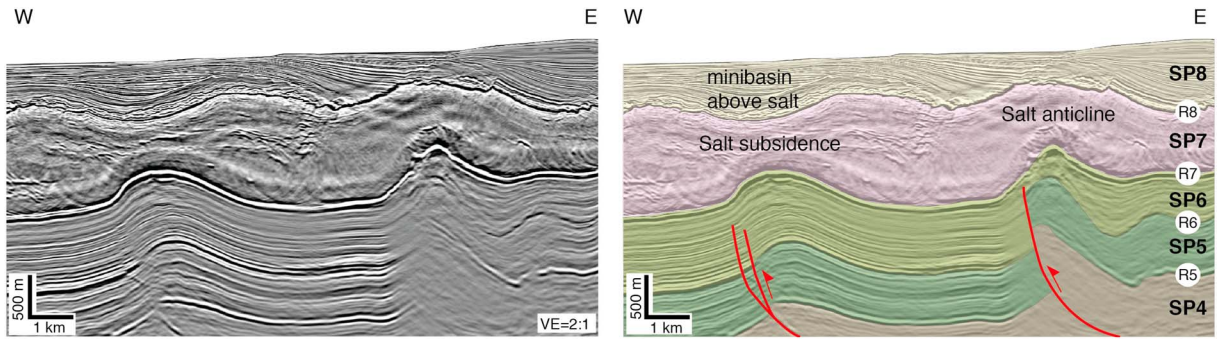

Figure 16. Seismic profile offshore central Lebanon from MC3D-LEB2012 PSDM seismic cube showing the occurrence of salt anticline and subsidence above two adjacent Miocene anticlinal structures. The occurrence of the Messinian evaporites, decoupling subsalt and suprasalt deformation, is challenging to determine continuous activity of structures. For location, see Figure 5.

Tripoli Thrusts (Figures 12 and 13) are inverted, we believe they are likely crustal structures linked to the evolution of Mount Lebanon. The timing of Beirut Thrust is lower Tertiary, based on the thickness variation of Eocene units along the fault plane (Figures 12). Beirut Thrust could be the offshore continuation of the Roum fault, which shows a similar timing and evolution [*Dubertret*, 1955; *Butler et al.*, 1998; *Nemer and Meghraoui*, 2006]

The determination of the accurate timing of activity of Tripoli Thrust has proved to be challenging. The large vertical displacement recorded in the pre-Tertiary units and the erosion of a large part of the Upper Cretaceous (Figure 13) insinuate that the Tripoli fault was an already existing structure prior to the Tertiary, and it continued to grow during the Miocene.

5.4. Late Miocene Pre-Messinian Deformation

The material presented in this paper suggests that offshore anticlines and strike-slip faults have been deformed immediately prior to the Messinian. This is demonstrated by (i) the absence of growth strata and angular unconformities in the Miocene units of these structures (Figures 9–14) and (ii) local erosion and truncation at the overlying base Messinian horizon (Figures 10–15). If the anticlines were folded in large part during the Early or late Miocene, then we would expect to find growth folding or drape sequences in these units. The fact that the top of the anticlines is capped by an erosive surface signifies that the deformation is immediately pre-Messinian.

At the onset of the Messinian, major geodynamic changes occurred in the eastern Mediterranean region. The northward propagation, development, and first phase of movement along the LFS took place in the mid-Miocene [*Freund et al.*, 1970; *Garfunkel*, 1981; *Quennell*, 1984] with the transpressive activity along the Lebanese restraining bend initiating in the late Miocene [*Butler et al.*, 1998; *Walley*, 1998; *Gomez et al.*, 2007b; *Homberg et al.*, 2010]. The northward propagation of the LFS during the middle to late Miocene was a direct response to rifting and seafloor spreading along the newly formed Red Sea [*Cochran*, 1983; *D'Acremont et al.*, 2005; *Fournier et al.*, 2010]. In the Levant Basin, the deformation, documented in this paper along anticlines and strike-slip faults starting immediately before the Messinian (Figure 17), correlates well with this major reorganization.

5.5. Post-Messinian Tectonics

It is difficult to determine if many of the interpreted Oligocene-Miocene structures are currently active using seismic data alone. Yet 3-D seismic data interpretation allowed providing evidence for local Pliocene uplift—i.e., current activity—along ENE-WSW faults (e.g., F1, F3, and F4; Figures 4, 10, and 11). One of these faults (F3) is associated with a cluster of earthquake epicenters (www.cnrs.edu.lb), confirming ongoing deformation. This fault is believed to be an offshore extension of the Douma ENE-WSW striking fault (Figure 3), which is also known for being seismically active [*Gedeon*, 1999]. Consequently, most of the observed ENE-WSW striking strike-slip faults are believed to be currently active. Due to the decoupling effect of the thick Messinian salt (Figure 16), it is hard to determine whether the other investigated structures are also still active.

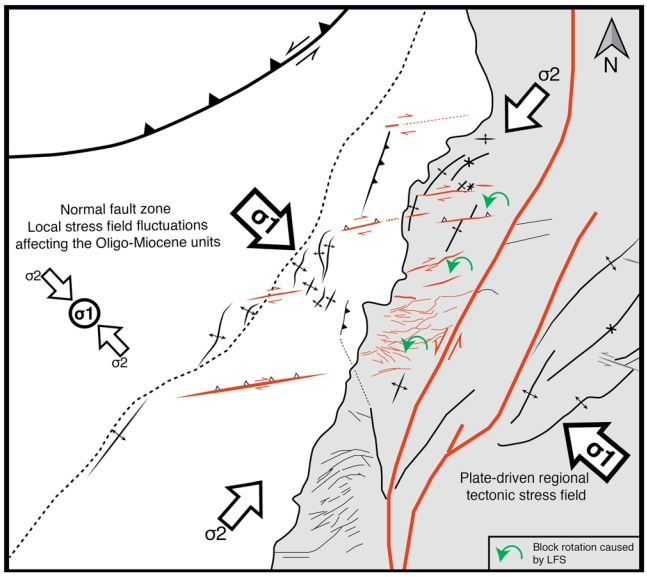

Figure 17. Sketch summarizing the results of this study in the Levant Basin offshore Lebanon. The faults in red are the structures that show evidence of current activity, including offshore ENE-WSW dextral strike-slip faults (this study), onshore ENE-WSW latitudinal dextral strike-slip faults (referenced herein), and NE-SW sinistral strike-slip faults (referenced herein). In the first phase of LFS movement, all structures in this map were active. During the second phase of LFS in the Pliocene to present day, only the ENE-WSW dextral strike-slip faults were active and might be linked to block rotations caused by the continuous sinistral movement of the LFS in Lebanon. The occurrence of the NW-SE normal faults in the deep basin might not be caused by these regional geodynamics but rather to a local stress-field fluctuation affecting only the Oligocene-Miocene units.

The structural map presented in Figure 3, together with the age constraints provided by the seismic-stratigraphic and earthquakes records, can be used to propose two tectonic scenarios for the northern Levant Basin offshore Lebanon (Figure 17): (i) all structures are still active today, having their activity masked by the decoupling effect of Messinian salt, or (ii) only the ENE-WSW striking strike-slip faults are active, with the rest of the structures becoming dormant since the Messinian or Pliocene. We favor the second scenario, due to the lack of evidence to prove current activity for the remaining structures.

At regional scale, the asthenospheric flow below Anatolia and accelerated rollback of the subduction zone along the Hellenic-Cyprus arc during the Tortonian [*Le Pichon and Kreamer*, 2010] caused a westward extrusion of Anatolia during the Messinian and the Pliocene. The propagation of the North Anatolian Fault toward the Aegean facilitated the westward escape of Anatolia, which was followed by a decrease in the onshore LFS slip rate during its second phase of movement in the Pliocene [*Freund et al.*, 1970; *Quennell*, 1984; *Le Pichon and Gaulier*, 1988]. In the Levant Basin, the Lattakia Ridge System (Figure 1) was reactivated into a sinistral strike-slip regime during the Pliocene after a long period of thrusting and subduction [*Hall et al.*, 2005]. These regional events are coeval with the cessation of folding demonstrated offshore in this paper (Figure 17).

The continuous activity of the ENE-WSW striking dextral strike-slip faults might be related to the sinistral shear along the LFS, causing counterclockwise block rotations along latitudinal faults [*Ron et al.*, 1984; *Ron*, 1987]. In strike-slip restraining bends, progressive deformation causes the rotation of the rock volume within the bend, as it is commonly observed in scaled analogue models [*Mcclay and Bonora*, 2001; *Mitra and Paul*, 2011]. This has also been observed in the complex restraining step over systems of the San Andreas Fault in Southern California [*Dickinson*, 1996]. In general, where the basement is already faulted prior to such rotations, it is not surprising that these faults will be reactivated into strike-slip faults [*McKenzie and Jackson*, 1986]. We have shown that ENE-WSW striking faults, active from the onset of Messinian, reactivate preexisting structures located primarily along the Levant margin onshore and offshore (Figure 17). This extends the *Ron et al.*'s [1984] hypothesis to the offshore domain. In the Levant Basin offshore Lebanon, this deformation mode corresponds to the second phase of deformation along the LFS.

5.6. Strain Partitioning Along the LFS and Current Shortening

The southern and middle segments of the LFS have slipped by different amounts [*Beydoun*, 1999]. The total recorded horizontal displacement in Lebanon amounts to 20–25 km [*Dubertret*, 1972], in contrast with the total displacement of ≈100 km along the Dead Sea Transform in Israel [*Freund et al.*, 1970; *Quennell*, 1984]. From GPS measurements, the movement of Arabia relative to Africa amounts to 4–6 mm/a [*Wdowinski et al.*, 2004; *Mahmoud et al.*, 2005; *Reilinger et al.*, 2006]. The Yammouneh Fault zone accommodates 3–4 mm/a slip rate [*Walley*, 1988; *Westaway*, 2004; *Gomez et al.*, 2006], leaving 1–2 mm/a of the motion along the LFS to be accommodated by different structures [*Gomez et al.*, 2007a].

Gomez et al. [2007b] argued that the Yammouneh Fault only accommodates strike-slip displacement, while the shortening component accommodated through oblique plate motion within the restraining bend partitioned into strike-slip displacement and perpendicular convergence. They postulated, through geometric calculations on different structures of the restraining bend, a 17% horizontal shortening of Mount Lebanon, close to the 10–15% bulk shortening suggested by *Hancock and Atiya* [1979]. Hence the remaining shortening should be accommodated by other faults or structures, and the larger horizontal motion measurable south of Lebanon should be transmitted northward through Lebanon in another way. A suggestion was that the Palmyrides and the offshore domain were good candidates to accommodate parts of the missing displacement.

Carton et al. [2009] argue that an active fold and thrust belt exists along the Levant margin, incipient of a future subduction zone in the Levant Basin offshore Lebanon, which might accommodate all the shortening onshore. On the other hand, *Homberg et al.* [2010] pointed to the absence of regional significant post-Miocene shortening onshore, questioning the magnitude of transpression during this time.

We have proved in this paper that the Levant Basin offshore Lebanon does not contain large strike-slip faults parallel to the restraining bend that could accommodate part of the LFS displacement. In addition, we find no evidence for current folding and deformation, since most of the structures are currently inactive. We therefore believe that the Levant Basin offshore Lebanon does not accommodate part of the shortening of the Lebanese restraining bend and other models should be developed to solve this controversial geologic question. Based on our observations, only the ENE-WSW striking dextral strike-slip faults provide evidence of current activity, as they accommodate the counterclockwise block rotations in Lebanon caused by the transpressive deformation of the LFS.

6. Conclusions

Based on the analysis of 3-D seismic reflection data in the Levant Basin offshore Lebanon, a variety of structures were investigated in detail consisting of the following:

1. Thick-skinned Late Cretaceous or early Tertiary NNE-SSW striking thrust faults found offshore Tripoli and Beirut. They do not show any evidence of present-day activity.
2. Thin-skinned NW-SE striking early Miocene normal faults found in the deeper part of the basin in the Oligocene-Miocene unit only. Their timing, orientation, and localization indicate a nontectonic control on their origin.
3. Thick-skinned ENE-WSW striking dextral strike-slip faults. These structures are inherited from Mesozoic extension and reactivated during the late Miocene immediately prior to the Messinian event. They are the only structures in the basin that provide evidence for continuous present-day activity and might be caused by the counterclockwise block rotation onshore triggered by the LFS movement.
4. NNE trending anticlines folded immediately prior to the Messinian event and overlying existing Late Cretaceous to early Tertiary structuration in the basin. These anticlines do not provide evidence for present-day deformation and are inactive currently.

This paper provides a good example of the impact of the evolution of plate boundaries on adjacent basins. The first stage of LFS propagation during late Miocene is associated with the onset of folding and ENE-WSW strike slip faulting in the basin, while the second in the Pliocene corresponds to the cessation of folding and dominance of ENE-WSW strike-slip faulting only.

In the absence of evidence for current shortening in the Levant Basin offshore Lebanon and the nonexisting large sinistral strike-slip faults in the basin parallel to the LFS trend, we advocate that the Lebanese restraining bend is mainly contained along the margin. Hence, the missing shortening and displacement of LFS cannot be found offshore.

Acknowledgments
The authors would like to acknowledge TOTAL, IFPEN, and UPMC for funding this project. The Lebanese Ministry of Energy and Water and the Lebanese Petroleum Administration are thanked for their support. Petroleum Geo-Services (PGS) is acknowledged for providing the data set and in particular Per Helge Semb for his help and cooperation. Lucien Montadert (Beicip-Franlab) is very much thanked for the discussions and his regional insight on the Mediterranean geology. Christopher A.L. Jackson, an anonymous reviewer, and Editor Claudio Faccenna are thanked for their thoughtful and constructive reviews, which greatly improved the manuscript.

References

Agudelo, W., J. F. Gamboa, S. Guevara, C. Piedratha, L. E. Rojas, M. Morales, and H. Alfonso (2009), Combining PSDM and Seismic Modeling to reduce uncertainties in time structural interpretation, in *X Simposio Bolivariano Exploracion Petrolera*, pp. 1–3, ACGGP Asociacion Colombiana de Geologos y Geofisicos del Petroleo, Cartagena, Columbia.

Allen, M. B., J. Jackson, and R. Walker (2004), Late Cenozoic reorganization of the Arabia-Eurasia collision and the comparison of short-term and long-term deformation rates, *Tectonics*, *23*, doi:10.1029/2003TC001530.

Bahorich, M., and S. Farmer (1995), 3D seismic discontinuity for faults and stratigraphic features: The coherence cube, *Leading edge*, 1053–1058.

Barrier, É., and B. Vrielynck (2008), Paleotectonic maps of the Middle East: Tectono-sedimentary-palinspatic maps from Late Norian to Pliocene, 14 maps, Commission de la carte geologique du monde.
Ben-Avraham, Z., A. Ginzburg, J. Makris, and L. Eppelbaum (2002), Crustal structure of the Levant Basin, eastern Mediterranean, *Tectonophysics*, *346*(1-2), 23–43, doi:10.1016/S0040-1951(01)00226-8.
Best, J. A., M. Barazangi, D. Al-Saad, T. Sawaf, and A. Gebran (1993), Continental margin evolution of the Northern Arabian Platform in Syria, *Am. Assoc. Pet. Geol. Bull.*, *77*(2), 173–193.
Beydoun, Z. R. (1977), Petroleum Prospects of Lebanon: Reevaluation, *Am. Assoc. Pet. Geol. Bull.*, *61*(I), 43–64, doi:10.1306/C1EA3BF4-16C9-11D7-8645000102C1865D.
Beydoun, Z. R. (1993), Evolution of the northeastern arabian plate margin and shelf: Hydrocarbon habitat and conceptual future potential, *Rev. Inst. Fr. Pet.*, *48*(4), 311–345.
Beydoun, Z. R. (1999), Evolution and development of the Levant (Dead Sea Rift) Transform System: A historical-chronological review of a structural controversy, in *Continental Tectonics*, edited by C. Mac Niocaill and P. D. Ryan, *Geol. Soc. London Spec. Publ.*, *164*, 239–255.
Bonini, M., F. Sani, and B. Antonielli (2012), Basin inversion and contractional reactivation of inherited normal faults: A review based on previous and new experimental models, *Tectonophysics*, *522-523*, 55–88, doi:10.1016/j.tecto.2011.11.014.
Boudagher-fadel, M., and G. N. Clark (2006), Stratigraphy, paleoenvironment and paleogeography of Maritime Lebanon: A key to Eastern Mediterranean Cenozoic history, *Stratigraphy*, *3*(2), 1–38.
Brew, G. E., M. Barazangi, A. K. Al-Maleh, and T. Sawaf (2001), Tectonic and Geologic Evolution of Syria, *GeoArabia*, *6*(4), 573–616.
Butler, R. W. H., S. Spencer, and H. M. Griffiths (1998), The structural response to evolving plate kinematics during transpression: Evolution of the Lebanese restraining bend of the Dead Sea Transform, in *Continental Transpressional and Transtensional Tectonics*, edited by R. E. Holdsworth, R. A. Strachan, and J. F. Dewey, *Geol. Soc. London Spec. Publ.*, *135*, 81–106.
Carton, H., et al. (2009), Seismic evidence for Neogene and active shortening offshore of Lebanon (Shalimar cruise), *J. Geophys. Res.*, *114*, B07407, doi:10.1029/2007JB005391.
Cartwright, J. A. (2011), Diagenetically induced shear failure of fine-grained sediments and the development of polygonal fault systems, *Mar. Pet. Geol.*, *28*(9), 1593–1610, doi:10.1016/j.marpetgeo.2011.06.004.
Cartwright, J. A., R. Bouroullec, D. James, and H. Johnson (1998), Polycyclic motion history of some Gulf Coast growth faults from high-resolution displacement analysis, *Geology*, *26*(9), 819–822, doi:10.1130/0091-7613(1998)026<0819.
Chaimov, T. A., M. Barazangi, D. Al-Saad, T. Sawaf, and A. Gebran (1992), Mesozoic and Cenozoic deformation inferred from seismic stratigraphy in the southwestern intracontinental Palmyride fold-thrust belt, Syria, *Geol. Soc. Am. Bull.*, *104*(6), 704–715, doi:10.1130/0016-7606(1992)104<0704:MACDIF>2.3.CO;2.
Chaimov, T. A., M. Barazangi, D. Al-Saad, T. Sawaf, and M. Khaddour (1993), Seismic fabric and 3-D structure of the southwestern intracontinental Palmyride fold belt, Syria, *Am. Assoc. Pet. Geol. Bull.*, *77*(12), 2032–2047.
Cochran, J. R. (1983), A Model for Development of Red Sea, *Am. Assoc. Pet. Geol. Bull.*, *67*(1), 41–69.
Cunningham, W. D., and P. Mann (2007), Tectonics of strike-slip restraining and releasing bends, *Geol. Soc. London Spec. Publ.*, *290*(1), 1–12, doi:10.1144/SP290.1.
D'Acremont, E., S. Leroy, M.-O. Beslier, N. Bellahsen, M. Fournier, C. Robin, M. Maia, and P. Gente (2005), Structure and evolution of the eastern Gulf of Aden conjugate margins from seismic reflection data, *Geophys. J. Int.*, *160*(3), 869–890, doi:10.1111/j.1365-246X.2005.02524.x.
Dewey, J. F., W. C. I. Pitman, W. B. F. Ryan, and J. Bonin (1973), Plate Tectonics and the Evolution of the Alpine System, *Geol. Soc. Am. Bull.*, *84*, 3137–3180, doi:10.1130/0016-7606(1973)84<3137.
Dickinson, W. R. (1996), Kinematics of transrotational tectonism in the California Transverse Ranges and its contribution to cumulative slip along the San Andreas transform fault system, *Geol. Soc. Am.*, *305*, 1–46, doi:10.1130/0-8137-2305-1.1.
Dooley, T. P., and G. Schreurs (2012), Analogue modelling of intraplate strike-slip tectonics: A review and new experimental results, *Tectonophysics*, *574-575*, 1–71, doi:10.1016/j.tecto.2012.05.030.
Druckman, Y. (1981), Comments on the structural reversal model as a factor of the geological evolution of Israel, *Isr. J. Earth Sci.*, *30*, 44–48.
Druckman, Y. (1984), Evidence for Early-Middle Triassic faulting and possible rifting from the Helez Deep Borehole in the coastal plain of Israel, in *The Geological Evolution of the Eastern Mediterranean*, edited by J. E. Dixon and A. H. F. Robertson, *Geol. Soc. London Spec. Publ.*, *17*, 203–212.
Druckman, Y., B. Buchbinder, G. M. Martinotti, R. Siman Tov, and P. Aharon (1995), The buried Afiq Canyon (eastern Mediterranean, Israel): A case study of a Tertiary submarine canyon exposed in Late Messinian times, *Mar. Geol.*, *123*, 167–185.
Dubertret, L. (1955), Carte géologique du Liban avec notices explicatives. Scale 1:200000, Ministry of public works, Lebanon.
Dubertret, L. (1972), Sur la dislocation de l'ancienne plaque sialique afrique sinai peninsule arabique.pdf, *Notes Mem. sur le Moyen Orient*, *12*(2), 227–243.
Dupin, I., J. Brahami, Y. Gou, and L. Montadert (2012), Petroleum assessment of the offshore Lebanon based on the seismic interpretation and the regional geological framework, paper presented at Lebanon International Petroleum Exploration forum and exhibition, Ministry of energy and water, Beirut.
Elias, A., et al. (2007), Active thrusting offshore Mount Lebanon: Source of the tsunamigenic A.D. 551 Beirut-Tripoli earthquake, *Geology*, *35*(8), 755–758, doi:10.1130/G23631A.1.
Eyal, Y. (1996), Stress field fluctuations along the Dead Sea rift since the Middle Miocene, *Tectonics*, *15*(1), 157–170, doi:10.1029/95TC02619.
Fournier, M., et al. (2010), Arabia-Somalia plate kinematics, evolution of the Aden-Owen-Carlsberg triple junction, and opening of the Gulf of Aden, *J. Geophys. Res.*, *115*, B04102, doi:10.1029/2008JB006257.
Freund, R. (1965), A model of the structural development of Israel and adjacent areas since Upper Cretaceous times, *Geol. Mag.*, *102*(3), 189–205.
Freund, R. (1974), Kinematics of transform and transcurrent faults, *Tectonophysics*, *21*, 93–134.
Freund, R., Z. Garfunkel, I. Zak, M. Goldberg, T. Weissbrod, B. Derin, F. Bender, F. E. Wellings, and R. W. Girdler (1970), The Shear along the Dead Sea Rift [and Discussion], *Philos. Trans. R. Soc. A Math. Phys. Eng. Sci.*, *267*(1181), 107–130, doi:10.1098/rsta.1970.0027.
Frizon de Lamotte, D., C. Raulin, N. Mouchot, J. Christophe, W. Daveau, C. Blanpied, and J. C. Ringenbach (2011), The southernmost margin of the Tethys realm during the Mesozoic and Cenozoic: Initial geometry and timing of the inversion processes, *Tectonics*, *30*, 1–22, doi:10.1029/2010TC002691.
Gardosh, M., and Y. Druckman (2006), Seismic stratigraphy, structure and tectonic evolution of the Levantine Basin, offshore Israel, in *Tectonic Development of the Eastern Mediterranean Region*, edited by A. H. F. Robertson and D. Mountrakis, *Geol. Soc. London Spec. Publ.*, *260*, 201–227.
Gardosh, M., Y. Druckman, B. Buchbinder, and M. Rybakov (2006), *The Levant Basin Offshore Israel: Stratigraphy, Structure, Tectonic Evolution and Implications for Hydrocarbon Exploration*, Geophysical Institute of Israel, pp. 1–119.

Gardosh, M., Z. Garfunkel, Y. Druckman, and B. Buchbinder (2010), Tethyan rifting in the Levant Region and its role in Early Mesozoic crustal evolution, in *Evolution of the Levant Margin and Western Arabia Platform Since the Mesozoic*, edited by C. Homberg and M. Bachmann, *Geol. Soc. London Spec. Publ.*, *341*, 9–36.

Garfunkel, Z. (1981), Internal structure of the Dead Sea leacky transform (rift) in relation to plate kinematics, *Tectonophysics*, *80*, 81–108, doi:10.1016/0040-1951(81)90143-8.

Garfunkel, Z. (1998), Constrains on the origin and history of the Eastern Mediterranean basin, *Tectonophysics*, *298*(1-3), 5–35, doi:10.1016/S0040-1951(98)00176-0.

Garfunkel, Z. (2004), Origin of the Eastern Mediterranean basin: A reevaluation, *Tectonophysics*, *391*(1-4), 11–34, doi:10.1016/j.tecto.2004.07.006.

Garfunkel, Z., and B. Derin (1984), Permian-early Mesozoic tectonism and continental margin formation in Israel and its implications for the history of the Eastern Mediterranean, in *The Geological Evolution of the Eastern Mediterranean*, edited by R. J. Dixon and A. H. F. Robertson, *Geol. Soc. London Spec. Publ.*, *17*, 187–201.

Gedeon, M. (1999), Structural analysis of latitudinal faults in the Mount Lebanon north of Beirut: Their kinematic and their role in the tectonic evolution of Lebanon MS thesis, Department of geology, American Univ. of Beirut, Beirut.

Gomez, F., M. Khawlie, C. Tabet, A. N. Darkal, K. Khair, and M. Barazangi (2006), Late Cenozoic uplift along the northern Dead Sea transform in Lebanon and Syria, *Earth Planet. Sci. Lett.*, *241*(3-4), 913–931, doi:10.1016/j.epsl.2005.10.029.

Gomez, F., G. Karam, M. Khawlie, S. McClusky, P. Vernant, R. Reilinger, R. Jaafar, C. Tabet, K. Khair, and M. Barazangi (2007a), Global Positioning System measurements of strain accumulation and slip transfer through the restraining bend along the Dead Sea fault system in Lebanon, *Geophys. J. Int.*, *168*(3), 1021–1028, doi:10.1111/j.1365-246X.2006.03328.x.

Gomez, F., T. Nemer, C. Tabet, M. Khawlie, M. Meghraoui, and M. Barazangi (2007b), Strain partitioning of active transpression within the Lebanese restraining bend of the Dead Sea Fault (Lebanon and SW Syria), in *Tectonics of Strike-Slip Restraining and Releasing Bends*, edited by W. D. Cunningham and P. Mann, *Geol. Soc. London Spec. Publ.*, *290*, 285–303.

Hall, J. T., T. J. Calon, A. E. Aksu, and S. R. Meade (2005), Structural evolution of the Latakia Ridge and Cyprus Basin at the front of the Cyprus Arc, Eastern Mediterranean Sea, *Mar. Geol.*, *221*, 261–297, doi:10.1016/j.margeo.2005.03.007.

Hancock, P. L., and M. S. Atiya (1979), Tectonic significance of mesofracture systems associated with the Lebanese segment of the Dead Sea transform fault, *J. Struct. Geol.*, *1*(2), 143–153, doi:10.1016/0191-8141(79)90051-8.

Hawie, N., R. Deschamps, F. H. Nader, C. Gorini, C. Müller, D. Desmares, A. Hoteit, D. Granjeon, L. Montadert, and F. Baudin (2013a), Sedimentological and stratigraphic evolution of northern Lebanon since the Late Cretaceous: Implications for the Levant margin and basin, *Arabian J. Geosci.*, doi:10.1007/s12517-013-0914-5.

Hawie, N., C. Gorini, R. Deschamps, F. H. Nader, L. Montadert, D. Granjeon, and F. Baudin (2013b), Tectono-stratigraphic evolution of the northern Levant Basin (offshore Lebanon), *Mar. Pet. Geol.*, *48*, 392–410, doi:10.1016/j.marpetgeo.2013.08.004.

Hempton, M. R. (1987), Constraints on Arabian Plate motion and extensional history of the Red Sea, *Tectonics*, *6*(6), 687–705, doi:10.1029/TC006i006p00687.

Hirsch, F., A. Flexer, A. Rosenfeld, and A. Yellin-Dror (1995), Palinspastic and crustal setting of the eastern Mediterranean, *J. Pet. Geol.*, *18*(2), 149–170.

Homberg, C., É. Barrier, M. Mroueh, C. Müller, W. Hamdan, and F. Higazi (2010), Tectonic evolution of the central Levant domain (Lebanon) since Mesozoic time, in *Evolution of the Levant Margin and Western Arabia Platform Since the Mesozoic*, edited by C. Homberg and M. Bachmann, *Geol. Soc. London Spec. Publ.*, *341*, 245–268.

Hsu, K. J., W. B. F. Ryan, and M. B. Cita (1973), Late miocene desiccation of the mediterranean, *Nature*, *242*, 240–244.

Khair, K., G. N. Tsokas, and T. Sawaf (1997), Crustal structure of the northern Levant region: Multiple source Werner deconvolution estimates for Bouguer gravity anomalies, *Geophys. J. Int.*, *128*(3), 605–616, doi:10.1111/j.1365-246X.1997.tb05322.x.

Le Pichon, X., and J.-M. Gaulier (1988), The rotation of Arabia and the Levant fault system, *Tectonophysics*, *153*(1-4), 271–294, doi:10.1016/0040-1951(88)90020-0.

Le Pichon, X., and C. Kreamer (2010), The miocene-to-present kinematic evolution of the eastern mediterranean and Middle East and its implications for dynamics, *Annu. Rev. Earth Planet. Sci.*, *38*, 323–351, doi:10.1146/annurev-earth-040809-152419.

Litak, R. K., M. Barazangi, G. E. Brew, T. Sawaf, A. Al-imam, and W. Al-Youssef (1998), Structure and evolution of the petroliferous euphrates graben system, Southeast Syria, *Am. Assoc. Pet. Geol. Bull.*, *82*(6), 1173–1190.

Lundin, E. R. (1992), Thin-skinned extensional tectonics on a salt detachment, northern Kwanza Basin, Angola, *Mar. Pet. Geol.*, *9*(4), 405–411.

Mahmoud, S., R. Reilinger, S. Mcclusky, P. Vernant, and A. Tealeb (2005), GPS evidence for northward motion of the Sinai Block: Implications for E. Mediterranean tectonics, *Earth Planet. Sci. Lett.*, *238*, 217–224, doi:10.1016/j.epsl.2005.06.063.

Makris, J., Z. Ben-Avraham, A. Behle, A. Ginzburg, P. Giese, L. Steinmetz, R. B. Whitmarsh, and S. Eleftheriou (1983), Seismic refraction profiles between Cyprus and Israel and their interpretation, *Geophys. J. Int.*, *75*, 575–591.

Mann, P., M. R. Hempton, D. C. Bradley, and K. Burke (1983), Development of pull-apart basins, *J. Geol.*, *91*(5), 529–5541.

Mcclay, K. R., and M. Bonora (2001), Analog models of restraining stepovers in strike-slip fault systems, *Am. Assoc. Pet. Geol. Bull.*, *85*(2), 233–260.

McKenzie, D., and J. Jackson (1986), A block model of distributed deformation by faulting, *J. Geol. Soc. London*, *143*(2), 349–353, doi:10.1144/gsjgs.143.2.0349.

Mitra, S., and D. Paul (2011), Structural geometry and evolution of releasing and restraining bends: Insights from laser-scanned experimental models, *Am. Assoc. Pet. Geol. Bull.*, *95*(7), 1147–1180, doi:10.1306/09271010060.

Montadert, L., P. H. Semb, O. Lie, and S. Kassinis (2010), New seismic may put offshore Cyprus hydrocarbon prospects in the spotlight, *First Break*, *28*(4), 91–101.

Montadert, L., S. Nicolaides, P. H. Semb, and O. Lie (2013), Petroleum Systems offshore Cyprus, in *Petroleum Systems of the Tethyan Region*, edited by L. Marlow, C. Kendall, and L. Yose, *AAPG Spec. Publ.*, Tulsa, pp. 301–334.

Moustafa, A. R. J. (2010), Structural setting and tectonic evolution of North Sinai folds, Egypt, in *Evolution of the Levant Margin and Western Arabia Platform Since the Mesozoic*, edited by C. Homberg and M. Bachmann, *Geol. Soc. London Spec. Publ.*, *341*, 37–63.

Moustafa, A. R. J., and M. H. Khalil (1994), Rejuvenation of the eastern Mediterranean passive continental margin in northern and central Sinai: New data from the Themed Fault, *Geol. Mag.*, *131*(4), 435–448.

Nemer, T. (1999), The roum fault: extent and associated structures, MS thesis, Department of geology, American Univ. of Beirut, Beirut.

Nemer, T., and M. Meghraoui (2006), Evidence of coseismic ruptures along the Roum fault (Lebanon): A possible source for the AD 1837 earthquake, *J. Struct. Geol.*, *28*(8), 1483–1495, doi:10.1016/j.jsg.2006.03.038.

Netzeband, G., K. Gohl, C. Hübscher, Z. Ben-Avraham, G. A. Dehghani, D. Gajewski, and P. Liersch (2006), The Levantine Basin—Crustal structure and origin, *Tectonophysics*, *418*(3-4), 167–188, doi:10.1016/j.tecto.2006.01.001.

Quennell, A. M. (1958), The structural and geomorphic evolution of the Dead Sea rift, *Q. J. Geol. Soc.*, *114*(1-4), 1–24, doi:10.1144/gsjgs.114.1.0001.
Quennell, A. M. (1984), The Western Arabia rift system, *Geol. Soc. London Spec. Publ.*, *17*(1), 775–788, doi:10.1144/GSL.SP.1984.017.01.62.
Reilinger, R., et al. (2006), GPS constraints on continental deformation in the Africa-Arabia-Eurasia continental collision zone and implications for the dynamics of plate interactions, *J. Geophys. Res.*, *111*, B05411, doi:10.1029/2005JB004051.
Robertson, A. H. F. (1998), Mesozoic-Tertiary tectonic evolution of the Easternmost Mediterranean area: Integration of marine and land evidence, in *Proceedings of the Ocean Drilling Program*, Sci. Results, vol. 160, edited by A. H. F. Robertson et al., pp. 723–782, Ocean Drilling Program, College Station, Tex.
Ron, H. (1987), Deformation along the Yammuneh the restaining bend of the Dead Sea Transform: Paleomagnetic data and kinematic implications, *Tectonics*, *6*(5), 653–666, doi:10.1029/TC006i005p00653.
Ron, H., and Y. Eyal (1985), Intraplate deformation by block rotation and mesostructures along the Dead Sea transform, northern Israel, *Tectonics*, *4*(1), 85–105, doi:10.1029/TC004i001p00085.
Ron, H., R. Freund, Z. Garfunkel, and A. Nur (1984), Block rotation by strike-slip faulting: Structural and paleomagnetic evidence, *J. Geophys. Res.*, *89*(B7), 6256–6270, doi:10.1029/JB089iB07p06256.
Sabbagh, G. (1961), Stratigraphie et tectonique du liban generalites: Exemple de deux structures anticlinales, 122 pp., MS thesis, Faculte de Science de Grenoble, Grenoble, France.
Sawaf, T., G. E. Brew, R. K. Litak, and M. Barazangi (2001), Geologic evolution of the intraplate palmyride basin and euphrates fault system syria, in *Peri-Tethys Memoir 6: Peri-Tethyan rift/Wrench Basins and Passive Margins*, edited by P. A. Ziegler et al., pp. 441–467, Memoire du Museum National D'histoire Naturelle, Paris.
Segev, A., and M. Rybakov (2010), Effects of Cretaceous plume and convergence, and Early Tertiary tectonomagmatic quiescence on the central and southern Levant continental margin, *J. Geol. Soc. London*, *167*(4), 731–749, doi:10.1144/0016-76492009-118.
Sengor, A. M. C., and Y. Yilmaz (1981), Tethyan evolution of Turkey: A plate tectonic approach, *Tectonophysics*, *75*, 181–241.
Stampfli, G. M., and C. Hochard (2009), Plate Tectonics of the Alpine Realm, in *Ancient Orogens and Modern Analogues*, edited by J. B. Murphy, J. D. Keppie, and A. J. Hynes, *Geol. Soc. London Spec. Publ.*, *327*, 89–111.
Sylvester, A. G. (1988), Strike-slip faults, *Geol. Soc. Am.*, *100*(11), 1666–1703.
Vidal, N., J. Alvarez-Marron, and D. Klaeschen (2000), Internal configuration of the Levantine Basin from seismic reflection data (eastern Mediterranean), *Earth Planet. Sci. Lett.*, *180*, 77–89.
Walley, C. D. (1988), A braided strike-slip model for the northern continuation of the Dead Sea Fault and its implications for Levantine tectonics, *Tectonophysics*, *145*(1-2), 63–72, doi:10.1016/0040-1951(88)90316-2.
Walley, C. D. (1998), Some outstanding issues in the geology of Lebanon and their importance in the tectonic evolution of the Levantine region, *Tectonophysics*, *298*(1-3), 37–62, doi:10.1016/S0040-1951(98)00177-2.
Walsh, J. J., and J. Watterson (1988), Analysis of the relationship between displacements and dimensions of faults, *J. Struct. Geol.*, *10*(3), 239–247.
Wdowinski, S., Y. Bock, G. Baer, L. Prawirodirdjo, N. Bechor, S. Naaman, R. Knafo, Y. Forrai, and Y. Melzer (2004), GPS measurements of current crustal movements along the Dead Sea Fault, *J. Geophys. Res.*, *109*, B05403, doi:10.1029/2003JB002640.
Westaway, R. (2004), Kinematic consistency between the Dead Sea Fault Zone and the Neogene and Quaternary left-lateral faulting in SE Turkey, *Tectonophysics*, *391*, 203–237, doi:10.1016/j.tecto.2004.07.014.
Wiprut, D., and M. D. Zoback (2002), Fault reactivation, leakage potential, and hydrocarbon column heights in the northern North Sea, in *Hydrocarbon Seal Quantification*, edited by A. G. Koestler and R. Hunsdale, pp. 203–219, Elsevier, Amsterdam.
Woodcock, N. H. (1986), The role of strike-slit fault systems at plate boundaries, *Philos. Trans. R. Soc. London*, *317*(1539), 13–29.
Zoback, M. D. (1991), State of stress and crustal deformation along weak transform faults, *Philos. Trans. R. Soc. London, Ser. A*, *337*(1645), 141–150.